Phase locking of multi-helicity neoclassical tearing modes in tokamak plasmas

Richard Fitzpatrick

Citation: Physics of Plasmas (1994-present) **22**, 042514 (2015); doi: 10.1063/1.4919030
View online: http://dx.doi.org/10.1063/1.4919030
View Table of Contents: http://scitation.aip.org/content/aip/journal/pop/22/4?ver=pdfcov
Published by the AIP Publishing

Phase locking of multi-helicity neoclassical tearing modes in tokamak plasmas

Richard Fitzpatrick
Institute for Fusion Studies, University of Texas at Austin, Austin, Texas 78712, USA

(Received 10 February 2015; accepted 14 April 2015; published online 27 April 2015)

The attractive "hybrid" tokamak scenario combines comparatively high q_{95} operation with improved confinement compared with the conventional $H_{98,y2}$ scaling law. Somewhat unusually, hybrid discharges often exhibit multiple neoclassical tearing modes (NTMs) possessing different mode numbers. The various NTMs are eventually observed to phase lock to one another, giving rise to a significant flattening, or even an inversion, of the core toroidal plasma rotation profile. This behavior is highly undesirable because the loss of core plasma rotation is known to have a deleterious effect on plasma stability. This paper presents a simple, single-fluid, cylindrical model of the phase locking of two NTMs with different poloidal and toroidal mode numbers in a tokamak plasma. Such locking takes place via a combination of nonlinear three-wave coupling and conventional toroidal coupling. In accordance with experimental observations, the model predicts that there is a bifurcation to a phase-locked state when the frequency mismatch between the modes is reduced to one half of its original value. In further accordance, the phase-locked state is characterized by the permanent alignment of one of the X-points of NTM island chains on the outboard midplane of the plasma, and a modified toroidal angular velocity profile, interior to the outermost coupled rational surface, which is such that the core rotation is flattened, or even inverted. © *2015 AIP Publishing LLC*. [http://dx.doi.org/10.1063/1.4919030]

I. INTRODUCTION

A magnetic confinement device is designed to trap a thermonuclear plasma on a set of toroidally nested magnetic flux-surfaces. Heat and particles flow around flux-surfaces relatively rapidly due to the free streaming of charged particles along magnetic field-lines. On the other hand, heat and particles are only able to diffuse across flux-surfaces relatively slowly, assuming that the magnetic field-strength is sufficiently high to render the particle gyroradii much smaller than the minor radius of the device. This article will concentrate on the *tokamak*, which is a type of toroidally axisymmetric magnetic confinement device in which the magnetic field is dominated by an approximately uniform toroidal component whose energy density is much larger than that of the plasma.[1]

Tokamak plasmas are subject to a number of macroscopic instabilities that limit their effectiveness. Such instabilities can be divided into two broad classes. So-called *ideal instabilities* are non-reconnecting modes that disrupt the plasma in a matter of microseconds.[2] However, such instabilities can usually be avoided by limiting the plasma pressure and/or by tailoring the toroidal current profile.[3] *Tearing modes*, on the other hand, are relatively slowly growing instabilities that are more difficult to prevent.[3,4] These instabilities tend to saturate at relatively low levels,[5–8] in the process reconnecting magnetic flux-surfaces to form helical structures known as *magnetic islands*. Magnetic islands are radially localized structures centered on so-called rational flux-surfaces that satisfy $\mathbf{k}\cdot\mathbf{B}=0$, where $\mathbf{k}$ is the wave vector of the instability, and $\mathbf{B}$ is the equilibrium magnetic field. Magnetic islands degrade plasma confinement because they enable heat and particles to flow very rapidly along field-lines from their inner to their outer radii, implying an almost complete loss of confinement in the region lying between these radii.[9]

Conventional tearing modes are driven unstable by inductive current gradients within the plasma and are relatively straight-forward to avoid in non-pathological tokamak discharges.[3] On the other hand, so-called *neoclassical tearing modes* are driven unstable by the perturbed bootstrap current[10,11] and are virtually impossible to avoid in high-β discharges.[12] Neoclassical tearing modes are conveniently classified in terms of the poloidal and toroidal mode numbers, m and n, respectively, of the associated magnetic island chains. The mode numbers of neoclassical tearing modes typically observed in high-β tokamak discharges are $m,n=5,4$; 4, 3; 3, 2; and 2, 1.[13] Note, however, that neoclassical tearing modes with different mode numbers do not usually occur simultaneously in such discharges.[13–16] In other words, the presence of a 5, 4 neoclassical tearing mode usually implies the absence of a 4, 3 mode, and vice versa.

The so-called *hybrid scenario* combines comparatively high q_{95} operation with improved confinement compared with the conventional $H_{98,y2}$ scaling law.[17,18] If this scenario could be reproduced on ITER then it would enable high-Q operation at reduced plasma current, which would be highly advantageous.[19,20] Somewhat unusually, hybrid discharges often exhibit multiple neoclassical tearing modes possessing different mode numbers. For example, 2, 1 and 3, 2 neoclassical modes have been observed simultaneously in both DIII-D and JET hybrid discharges.[21,22] In addition, 4, 3 and 5, 4 modes have been observed simultaneously in JET hybrid discharges.[23] In all cases, the various modes are eventually

observed to phase lock to one another, giving rise to a significant flattening, or even an inversion, of the core toroidal plasma rotation profile.[22,23] This behavior is highly undesirable because the loss of core plasma rotation is known to have a deleterious effect on plasma stability (because it facilitates locked mode formation).

The aim of this paper is to present a simple, single-fluid, cylindrical model of the phase locking of two neoclassical tearing modes with different poloidal and toroidal mode numbers in a tokamak plasma. Such locking takes place via a combination of nonlinear three-wave coupling[24–26] and conventional toroidal coupling.[27–29] It is of particular interest to establish the final phase relation of the phase-locked islands, as well as the effect of the phase locking on the plasma toroidal rotation profile.

This paper is organized as follows. In Sec. II, we introduce the fundamental building blocks of our theory. In Sec. III, we describe a simple model plasma equilibrium that is adopted in this paper to facilitate calculations. In Sec. IV, we analyze the nonlinear three-wave coupling of three neoclassical tearing modes with different poloidal and toroidal mode numbers. In Sec. V, we describe the conventional toroidal coupling of two neoclassical tearing modes with a common toroidal mode number. In Sec. VI, we combine the analysis of Secs. IV and V to explain how two neoclassical tearing modes with different poloidal and toroidal mode numbers can phase lock to one another. In Sec. VII, we investigate the phase-locking thresholds associated with the three different phase-locking mechanisms discussed in Secs. IV–VI. Finally, we summarize the paper in Sec. VIII.

II. PRELIMINARY ANALYSIS

A. Plasma equilibrium

Consider a large-aspect-ratio tokamak plasma whose magnetic flux-surfaces map out almost concentric circles in the poloidal plane. Such a plasma is well approximated as a periodic cylinder. Suppose that the minor radius of the plasma is a. Let us adopt standard cylindrical coordinates: r, θ, z. The system is assumed to be periodic in the z-direction, with period $2\pi R_0$, where R_0 is the simulated plasma major radius. It is helpful to define the simulated toroidal angle $\phi = z/R_0$, as well as the normalized radial coordinate $\hat{r} = r/a$.

The equilibrium magnetic field is written

$$\mathbf{B} = B_\phi\,[0,\,\epsilon\,\hat{B}_\theta(\hat{r}),\,1], \tag{1}$$

where

$$\epsilon = \frac{a}{R_0} \ll 1, \tag{2}$$

is the inverse aspect-ratio of the plasma. Here, $B_\phi > 0$ is the (approximately uniform) toroidal magnetic field-strength. The equilibrium plasma current takes the form

$$\mu_0\,\mathbf{J} = \frac{B_\phi}{R_0}\,\big[0,\,0,\,\sigma(\hat{r})\big], \tag{3}$$

where

$$\sigma(\hat{r} \geq 1) = 0. \tag{4}$$

The function $\sigma(\hat{r})$ parameterizes the toroidal current profile. The safety-factor profile is defined

$$q(\hat{r}) = \frac{\hat{r}}{\hat{B}_\theta}. \tag{5}$$

Moreover, the safety-factor and current profiles are related via

$$\sigma(\hat{r}) = \frac{1}{\hat{r}}\frac{d}{d\hat{r}}\left(\frac{\hat{r}^{\,2}}{q}\right). \tag{6}$$

Note that a conventional tokamak plasma is characterized by a positive, monotonically increasing (in $\hat{r}$), $\mathcal{O}(1)$, safety-factor profile. This implies that $\sigma(\hat{r})$ is positive, monotonically decreasing, and $\mathcal{O}(1)$.

B. Magnetic perturbations

We can write the total magnetic field as

$$\mathbf{B}(\mathbf{r},t) = \nabla\psi(\mathbf{r},t)\times\mathbf{e}_z + B_\phi\,\mathbf{e}_z, \tag{7}$$

where

$$\psi(\mathbf{r},t) = \epsilon\,B_\phi\,a\,\psi^{\,0,0}(\hat{r}) + \epsilon\,B_\phi\,a\sum_{m,n}^{m>0}\psi^{\,m,n}(\hat{r},t)\,\mathrm{e}^{\,\mathrm{i}\,(m\,\theta - n\,\phi)}, \tag{8}$$

and $|\psi^{\,m,n}| \ll |\psi^{\,0,0}|$ for all $m, n \neq 0, 0$. This representation is valid as long as $m \gg n\,\epsilon$ for all $m, n \neq 0, 0$.[26]

For the special case of the 0, 0 harmonic, we have

$$\frac{d\psi^{\,0,0}}{d\hat{r}} = -\frac{\hat{r}}{q}. \tag{9}$$

For the other harmonics, the linearized equations of marginally stable, ideal-MHD, which govern small-amplitude, helical magnetic perturbations throughout virtually all of the plasma (and, also, in the vacuum region surrounding the plasma), yield[30]

$$\left(\frac{\partial^2}{\partial\hat{r}^{\,2}} + \frac{1}{\hat{r}}\frac{\partial}{\partial\hat{r}} - \frac{m^2}{\hat{r}^{\,2}}\right)\psi^{\,m,n} - \frac{m\,\sigma'}{F^{\,m,n}}\,\psi^{\,m,n} = 0, \tag{10}$$

where

$$F^{\,m,n}(\hat{r}) = \frac{\hat{r}}{q}\,(m - n\,q), \tag{11}$$

and $' \equiv d/d\hat{r}$. Close to the magnetic axis, the well-behaved solutions of Eq. (10) take the form

$$\psi^{\,m,n}(\hat{r},t) = A(t)\,\hat{r}^{\,m}, \tag{12}$$

where $A(t)$ is arbitrary. If we assume that there is a perfectly conducting wall at $r/a = b$, where $b \geq 1$, then the appropriate boundary condition at $\hat{r} = b$ is[30]

$$\psi^{\,m,n}(b,t) = 0. \tag{13}$$

C. Shafranov shift

We can simulate a small Shafranov shift of the magnetic flux-surfaces by applying a static, 1, 0 perturbation to the equilibrium. Thus, if

$$\psi(\hat{r},\theta) = \psi^{0,0}(\hat{r}) + \psi^{1,0}(\hat{r})\cos\theta, \tag{14}$$

then the Shafranov shift (normalized to a) is

$$\Delta(\hat{r},\theta) = \Delta^{1,0}(\hat{r})\cos\theta, \tag{15}$$

where

$$\Delta^{1,0}(\hat{r}) = -\frac{\psi^{1,0}(\hat{r})}{d\psi^{0,0}/d\hat{r}} = \frac{q(\hat{r})\,\psi^{1,0}(\hat{r})}{\hat{r}}. \tag{16}$$

It is convenient to normalize the $\psi^{1,0}(\hat{r})$ eigenfunction such that

$$\psi^{1,0}(\hat{r}) = \frac{\Delta_a^{1,0}}{q_a}\,\hat{\psi}^{1,0}(\hat{r}), \tag{17}$$

where $\hat{\psi}^{1,0}(\hat{r})$ and $\Delta_a^{1,0}$ are real, $q_a = q(1)$, and

$$\hat{\psi}^{1,0}(1) = 1. \tag{18}$$

It follows that $\Delta^{1,0}(1) = \Delta_a^{1,0}$. In other words, $\Delta_a^{1,0}$ is the Shafranov shift at the edge of the plasma. Assuming that $\Delta_a^{1,0} > 0$, the simulated outboard mid-plane of the plasma corresponds to $\theta = 0$ (because the Shafranov shift is in the direction of the outboard mid-plane in conventional tokamak plasmas[29]).

D. Rational surfaces

Equation (10) becomes singular at the rational surface, $\hat{r} = \hat{r}^{m,n}$, where

$$F^{m,n}(\hat{r}^{m,n}) = 0, \tag{19}$$

indicating a local breakdown of marginally stable, ideal-MHD.[4] Defining

$$x = \frac{\hat{r} - \hat{r}^{m,n}}{\hat{r}^{m,n}}, \tag{20}$$

the most general solution to Eq. (10) in the vicinity of the rational surface takes the form[26,29]

$$\psi^{m,n}(x,t) = C_L^{m,n}(t)[1 + \lambda^{m,n}\,x\,(\ln|x| - 1) + \cdots] + C_S^{m,n}(t)(x + \cdots), \tag{21}$$

where

$$\lambda^{m,n} = \left[\frac{m\,r\,(-\sigma')}{n\,s}\right]_{\hat{r}^{m,n}}, \tag{22}$$

and

$$s(\hat{r}) = \frac{\hat{r}}{q}\frac{dq}{d\hat{r}}. \tag{23}$$

According to conventional asymptotic matching theory, the coefficient of the large solution, $C_L^{m,n}$, must be the same on both sides of the rational surface, whereas the coefficient of the small solution, $C_S^{m,n}$, can be different on either side.[31] Let

$$\Psi^{m,n}(t) = C_L^{m,n}, \tag{24}$$

$$\Delta\Psi^{m,n}(t) = [C_S^{m,n}]_{\hat{r}^{m,n}_-}^{\hat{r}^{m,n}_+}. \tag{25}$$

Here, $\Psi^{m,n}(t)$ is the (normalized) reconnected magnetic flux at the rational surface, whereas $\Delta\Psi^{m,n}(t)$ parameterizes the strength of the m, n current sheet at the same surface.[30,32]

It is helpful to normalize resonant perturbations (i.e., perturbations with rational surfaces lying within the plasma) such that

$$\psi^{m,n}(\hat{r},t) = \Psi^{m,n}(t)\,\hat{\psi}^{m,n}(\hat{r}), \tag{26}$$

where

$$\hat{\psi}^{m,n}(0) = \hat{\psi}^{m,n}(b) = 0, \tag{27}$$

$$\hat{\psi}^{m,n}(\hat{r}^{m,n}) = 1, \tag{28}$$

and $\hat{\psi}^{m,n}(\hat{r})$ is real. The conventional tearing stability index for the m, n mode (i.e., Δ' normalized to the radius of the rational surface[4]) then becomes[29]

$$E^{m,n} = \left[\hat{r}\,\frac{d\hat{\psi}^{m,n}}{d\hat{r}}\right]_{\hat{r}^{m,n}_-}^{\hat{r}^{m,n}_+}. \tag{29}$$

Thus, if mode coupling effects are neglected then $\Delta\Psi^{m,n} = E^{m,n}\,\Psi^{m,n}$. Note that, for the sake of simplicity, we are neglecting any dependence of the stability index, $E^{m,n}$, on the island width.[6–8]

E. Nonlinear magnetic island physics

Let

$$\Psi^{m,n}(t) = \hat{\Psi}^{m,n}\,\mathrm{e}^{\,\mathrm{i}\,\varphi^{m,n}(t)}, \tag{30}$$

where $\hat{\Psi}^{m,n}(t)$ is real and positive, and $\varphi^{m,n}(t)$ is real. Making use of the well-known constant-ψ approximation,[4] which is valid provided that $|\Delta\Psi^{m,n}|\,W^{m,n} \ll |\Psi^{m,n}|$,[33] the reconnected magnetic flux at the m, n rational surface gives rise to a magnetic island chain whose full radial width (normalized to a) is

$$W^{m,n} = 4\left[\frac{\hat{\Psi}^{m,n}}{(n/m)\,s(\hat{r}^{m,n})}\right]^{1/2}. \tag{31}$$

The island X-points are located at angular positions that satisfy

$$m\,\theta - n\,\phi + \varphi^{m,n} = j\,2\pi, \tag{32}$$

where j is an integer (i.e., at positions where $\mathrm{Re}\{\psi^{m,n}(\hat{r}^{m,n},t)\,\exp[\mathrm{i}\,(m\,\theta - n\,\phi)]\}$ attains its maximum positive value). Likewise, the island O-points are located at

$$m\,\theta - n\,\phi + \varphi^{m,n} = (2j-1)\,\pi, \tag{33}$$

(i.e., at positions where $\mathrm{Re}\{\psi^{m,n}(\hat{r}^{m,n},t)\,\exp[\mathrm{i}\,(m\,\theta - n\,\phi)]\}$ attains its maximum negative value).

The well-known Rutherford island width evolution equation takes the form[5,11]

$$0.8227\,\tau_R^{m,n}\,\hat{r}^{\,m,n}\,\frac{dW^{\,m,n}}{dt} = \mathrm{Re}\left(\frac{\Delta\Psi^{\,m,n}}{\Psi^{\,m,n}}\right) - 9.25\,\frac{\sqrt{\epsilon\,\hat{r}^{\,m,n}}}{s^{\,m,n}} \times \left(\frac{m}{n\,\epsilon\,\hat{r}^{\,m,n}}\right)^2 \left(\frac{\mu_0\,\hat{r}\,p'}{B_\phi^2}\right)_{\hat{r}^{\,m,n}} \frac{\hat{r}^{\,m,n}}{W^{\,m,n}}, \tag{34}$$

where $s^{\,m,n} = s(\hat{r}^{\,m,n})$, and $\tau_R^{m,n} = (\mu_0\,a^2/\eta)_{\hat{r}^{\,m,n}}$ is the resistive evolution timescale at the m, n rational surface. Here, $\eta(\hat{r})$ is the plasma (parallel) resistivity profile, whereas $p(\hat{r})$ is the plasma pressure profile.

The final term on the right-hand side of Eq. (34) represents the destabilizing influence of the *perturbed bootstrap current*.[10] Here, we are assuming that the magnetic island width exceeds the threshold value required to flatten the pressure profile within the island's magnetic separatrix.[11] We are also assuming that the island width exceeds the ion banana width.[34] Note that the stabilizing effect of magnetic curvature (which is generally smaller than the destabilizing effect of the perturbed bootstrap current) is neglected in this paper.[35]

Finally, adopting the standard *no-slip* assumption (that a magnetic island chain is convected by the local plasma, which is effectively trapped within its magnetic separatrix),[30] we can write

$$\frac{d\varphi^{\,m,n}}{dt} = -m\,\Omega_\theta^{\,m,n} + n\,\Omega_\phi^{\,m,n}, \tag{35}$$

where $\Omega_\theta^{\,m,n} = \Omega_\theta(\hat{r}^{\,m,n},t)$ and $\Omega_\phi^{\,m,n} = \Omega_\phi(\hat{r}^{\,m,n},t)$. Here, $\Omega_\theta(\hat{r},t)$ and $\Omega_\phi(\hat{r},t)$ are the plasma poloidal and toroidal angular velocity profiles, respectively.

F. Toroidal torque balance

It is easily demonstrated that zero net toroidal electromagnetic torque can be exerted in any region of the plasma governed by the equations of marginally stable, ideal-MHD.[26,30] However, the equations of marginally stable, ideal-MHD break down in the immediate vicinities of the various rational surfaces inside the plasma. Hence, it is possible for localized torques to develop at these surfaces. The net toroidal electromagnetic torque that develops in the vicinity of the m, n rational surface is written[30,32]

$$\delta T_{\mathrm{EM}}^{m,n} = \frac{2\pi^2\,B_\phi^2\,a^4}{\mu_0\,R_0}\,\delta\hat{T}_{\mathrm{EM}}^{\,m,n}, \tag{36}$$

where

$$\delta\hat{T}_{\mathrm{EM}}^{\,m\,n} = n\,\mathrm{Im}[\Delta\Psi^{\,m,n}\,(\Psi^{\,m,n})^*]. \tag{37}$$

It is assumed that the poloidal velocity profile is fixed, due to the presence of strong *poloidal flow damping* in the plasma.[30,36] If $\Delta\Omega_\phi(\hat{r},t)$ is the modification to the plasma toroidal angular velocity profile caused by the localized electromagnetic torques acting at the various rational surfaces then we can write[30]

$$\rho\,a^2\,\frac{\partial\Delta\Omega_\phi}{\partial t} - \frac{1}{\hat{r}}\,\frac{\partial}{\partial\hat{r}}\left(\mu\,\hat{r}\,\frac{\partial\Delta\Omega_\phi}{\partial\hat{r}}\right) = 0, \tag{38}$$

where

$$\frac{\partial\Delta\Omega_\phi(0,t)}{\partial\hat{r}} = \Delta\Omega_\phi(1,t) = 0. \tag{39}$$

Here, $\rho(\hat{r})$ and $\mu(\hat{r})$ are the plasma mass density and (perpendicular) viscosity profiles, respectively. The localized viscous toroidal torque that develops at the m, n rational surface, as a consequence of the modification to the toroidal angular velocity profile, is[30]

$$\delta T_{\mathrm{VS}}^{m,n} = 4\pi^2\,R_0^3\left[\mu\,\hat{r}\,\frac{\partial\Delta\Omega_\phi}{\partial\hat{r}}\right]_{\hat{r}_-^{\,m,n}}^{\hat{r}_+^{\,m,n}}. \tag{40}$$

Torque balance at the m, n rational surface requires that[30,32]

$$\delta T_{\mathrm{EM}}^{m,n} + \delta T_{\mathrm{VS}}^{m,n} = 0, \tag{41}$$

which reduces to

$$\frac{2\,(\tau_H^{m,n})^2}{\epsilon^2\,\tau_M^{m,n}}\left[\hat{r}\,\frac{\partial\Delta\Omega_\phi}{\partial\hat{r}}\right]_{\hat{r}_-^{\,m,n}}^{\hat{r}_+^{\,m,n}} = -\delta\hat{T}_{\mathrm{EM}}^{\,m,n}, \tag{42}$$

where $\tau_H^{m,n} = (R_0\,\sqrt{\mu_0\,\rho}/B_\phi)_{\hat{r}^{\,m,n}}$ is the hydromagnetic timescale at the m, n rational surface, whereas $\tau_M^{m,n} = (a^2\,\rho/\mu)_{\hat{r}^{\,m,n}}$ is the corresponding momentum diffusion timescale.

G. Nonlinear coupling

Consider the nonlinear (i.e., emanating from the $\delta\mathbf{J}\times\delta\mathbf{B}$ term in the marginally stable, ideal-MHD, force-balance equation) coupling of the m_1, n_1, the m_2, n_2, and the m_3, n_3 modes. Of course, such coupling is only possible when the mode numbers satisfy the standard three-wave coupling constraint[24,25]

$$m_3 = m_1 + m_2, \tag{43}$$

$$n_3 = n_1 + n_2. \tag{44}$$

According to the analysis of Ref. 26 (adopting the conventional, large aspect-ratio, tokamak orderings $q\sim\mathcal{O}(1)$, $\epsilon\ll 1$, and $m\gg n\,\epsilon$), the coupling is such that

$$\Delta\Psi^{\,m_1,n_1} = E^{\,m_1,n_1}\,\Psi^{\,m_1,n_1} + \mathcal{C}_{m_1,m_2,m_3}^{n_1,n_2,n_3}\,(\Psi^{\,m_2,n_2})^*\,\Psi^{\,m_3,n_3}, \tag{45}$$

$$\Delta\Psi^{\,m_2,n_2} = E^{\,m_2,n_2}\,\Psi^{\,m_2,n_2} + \mathcal{C}_{m_1,m_2,m_3}^{n_1,n_2,n_3}\,(\Psi^{\,m_1,n_1})^*\,\Psi^{\,m_3,n_3}, \tag{46}$$

$$\Delta\Psi^{\,m_3,n_3} = E^{\,m_3,n_3}\,\Psi^{\,m_3,n_3} + \mathcal{C}_{m_1,m_2,m_3}^{n_1,n_2,n_3}\,\Psi^{\,m_1,n_1}\,\Psi^{\,m_2,n_2}, \tag{47}$$

where

$$\mathcal{C}^{n_1,n_2,n_3}_{m_1,m_2,m_3} = \int_0^1 t^{n_1,n_2,n_3}_{m_1,m_2,m_3}(\hat{r})\, d\hat{r}, \tag{48}$$

$$\begin{aligned} t^{n_1,n_2,n_3}_{m_1,m_2,m_3}(\hat{r}) = -\frac{\sigma'}{4}\Bigg[&\hat{r}\left(\hat{\psi}^{\,m_1,n_1}\right)'\hat{\psi}^{\,m_2,n_2}\,\hat{\psi}^{\,m_3,n_3}\,\frac{m_2\,m_3}{F^{\,m_2,n_2}\,F^{\,m_3,n_3}}\\ &+\hat{\psi}^{\,m_1,n_1}\,\hat{r}\left(\hat{\psi}^{\,m_2,n_2}\right)'\hat{\psi}^{\,m_3,n_3}\,\frac{m_1\,m_3}{F^{\,m_1,n_1}\,F^{\,m_3,n_3}}\\ &+\hat{\psi}^{\,m_1,n_1}\,\hat{\psi}^{\,m_2,n_2}\,\hat{r}\left(\hat{\psi}^{\,m_3,n_3}\right)'\frac{m_1\,m_2}{F^{\,m_1,n_1}\,F^{\,m_2,n_2}}\\ &+\hat{\psi}^{\,m_1,n_1}\,\hat{\psi}^{\,m_2,n_2}\,\hat{\psi}^{\,m_3,n_3}\,\frac{(\hat{r}/q)\,(2-\sigma\,q)}{F^{\,m_1,n_1}\,F^{\,m_2,n_2}\,F^{\,m_3,n_3}}\Bigg]. \end{aligned} \tag{49}$$

III. MODEL PLASMA EQUILIBRIUM

A. Current and safety-factor profiles

In the following, to facilitate calculations, we adopt a model plasma equilibrium in which

$$\sigma(\hat{r}) = \begin{cases} 2/q_0 & \hat{r} \le c \\ 0 & \hat{r} > c \end{cases}, \tag{50}$$

where $0 < c < 1$. It follows from Eq. (6) that

$$q(\hat{r}) = \begin{cases} q_0 & \hat{r} \le c \\ q_0\,(\hat{r}/c)^2 & \hat{r} > c \end{cases}, \tag{51}$$

from Eq. (23) that

$$s(\hat{r}) = \begin{cases} 0 & \hat{r} \le c \\ 2 & \hat{r} > c \end{cases}, \tag{52}$$

and from Eq. (11) that

$$F^{\,m,n}(c) = \frac{c}{q_0}\,(m - n\,q_0). \tag{53}$$

Furthermore

$$c = \left(\frac{q_0}{q_a}\right)^{1/2}, \tag{54}$$

and

$$\sigma'(\hat{r}) = -\frac{2}{q_0}\,\delta(\hat{r} - c). \tag{55}$$

B. Linearized, marginally stable, ideal-MHD equation

Equations (10), (26), (53), and (55) reduce to

$$\left(\frac{d^2}{d\hat{r}^{\,2}} + \frac{1}{\hat{r}}\,\frac{d}{d\hat{r}} - \frac{m^2}{\hat{r}^{\,2}}\right)\hat{\psi}^{\,m,n} = 0, \tag{56}$$

with

$$\left[\hat{r}\,\frac{d\hat{\psi}^{\,m,n}}{d\hat{r}}\right]_{c-}^{c+} = -\frac{2m}{(m - n\,q_0)}\,\hat{\psi}^{\,m,n}(c). \tag{57}$$

C. Shafranov shift

For the 1, 0 mode (which parameterizes the Shafranov shift of the equilibrium magnetic flux-surfaces), Eqs. (17), (18), (56), and (57) give

$$\hat{\psi}^{\,1,0}(\hat{r}) = \frac{\hat{r}}{c^{\,2}}, \tag{58}$$

for $0 \le \hat{r} \le c$, and

$$\hat{\psi}^{\,1,0}(\hat{r}) = \frac{1}{\hat{r}}, \tag{59}$$

for $c < \hat{r} \le 1$. Thus, it follows from Eqs. (16), (51), and (54) that

$$\Delta^{\,1,0}(\hat{r}) = \Delta^{\,1,0}_a. \tag{60}$$

In other words, the Shafranov shift is uniform across the plasma. It is also clear that

$$\hat{\psi}^{\,1,0}(c) = \frac{1}{c}, \tag{61}$$

and

$$\frac{1}{2}\left(\hat{r}\,\frac{d\hat{\psi}^{\,1,0}}{d\hat{r}}\bigg|_{c-} + \hat{r}\,\frac{d\hat{\psi}^{\,1,0}}{d\hat{r}}\bigg|_{c+}\right) = 0. \tag{62}$$

D. Eigenfunction of tearing mode

For a resonant mode, assuming that $c \le \hat{r}^{\,m,n} \le 1$, Eqs. (11), (19), (51), and (54) yield

$$\hat{r}^{\,m,n} = \left(\frac{m}{n\,q_a}\right)^{1/2}. \tag{63}$$

Furthermore, Eqs. (27), (28), (56), and (57) give

$$\hat{\psi}^{\,m,n}(\hat{r}) = \frac{(m - n\,q_0)\,(\hat{r}/c)^{+m}}{(m - 1 - n\,q_0)\,(\hat{r}^{\,m,n}/c)^{+m} + (\hat{r}^{\,m,n}/c)^{-m}}, \tag{64}$$

for $0 \le \hat{r} \le c$, and

$$\hat{\psi}^{\,m,n}(\hat{r}) = \frac{(m - 1 - n\,q_0)\,(\hat{r}/c)^{+m} + (\hat{r}/c)^{-m}}{(m - 1 - n\,q_0)\,(\hat{r}^{\,m,n}/c)^{+m} + (\hat{r}^{\,m,n}/c)^{-m}}, \tag{65}$$

for $c < \hat{r} \le \hat{r}^{\,m,n}$, and

$$\hat{\psi}^{\,m,n}(\hat{r}) = \frac{(\hat{r}/b)^{+m} - (\hat{r}/b)^{-m}}{(\hat{r}^{\,m,n}/b)^{+m} - (\hat{r}^{\,m,n}/b)^{-m}}, \tag{66}$$

for $\hat{r}^{\,m,n} < \hat{r} \le b$. It follows from Eqs. (29), (65), and (66) that

$$E^{\,m,n} = -2m\left(\frac{m - 1 - n\,q_0 + [q_0/q_b]^m}{\left[1 - (m/n\,q_b)^m\right]\left[m - 1 - n\,q_0 + (n\,q_0/m)^m\right]}\right), \tag{67}$$

where $q_b = q_a\,b^{\,2} = q(b)$. Note that $E^{\,1,n} = \infty$ for the special case of $m = 1$ internal-kink modes. For conventional $m > 1$

tearing modes, it is easily demonstrated that $E^{m,n} \leq 0$ provided

$$n\,q_0 \leq m - 1 + \left(\frac{q_0}{q_b}\right)^m. \tag{68}$$

Finally, it is also clear that

$$\hat{\psi}^{\,m,n}(c) = \frac{m - n\,q_0}{(m - 1 - n\,q_0)\,(m/n\,q_0)^{\,m/2} + (n\,q_0/m)^{\,m/2}}, \tag{69}$$

and

$$\frac{1}{2}\left(\hat{r}\,\frac{d\hat{\psi}^{\,m,n}}{d\hat{r}}\bigg|_{c-} + \hat{r}\,\frac{d\hat{\psi}^{\,m,n}}{d\hat{r}}\bigg|_{c+}\right) = \frac{m\,(m - 1 - n\,q_0)}{(m - n\,q_0)}\,\hat{\psi}^{\,m,n}(c). \tag{70}$$

IV. NONLINEAR COUPLING OF THREE NEOCLASSICAL TEARING MODES

A. Introduction

Consider the nonlinear coupling of three modes, resonant at three different rational surfaces within the plasma, whose mode numbers are m_1, n_1; m_2, n_2; and m_3, n_3, where $m_3 = m_1 + m_2$ and $n_3 = n_1 + n_2$. The fact that the modes are resonant implies that $n_1, n_2, n_3 > 0$. It is assumed that $m_1 \neq 1$ and $m_2 \neq 1$. In other words, none of the coupled modes are $m = 1$ internal-kink modes. It follows that the modes in question are all tearing modes. Without loss of generality, we can write $m_1/n_1 < m_2/n_2$, which implies that $m_1/n_1 < m_3/n_3 < m_2/n_2$. Hence, according to Eq. (63), $\hat{r}^{\,m_1,n_1} < \hat{r}^{\,m_3,n_3} < \hat{r}^{\,m_2,n_2}$. It is assumed that all three tearing modes are intrinsically stable—i.e., $E^{m_1,n_1}, E^{m_2,n_2}, E^{m_3,n_3} < 0$—but are maintained in the plasma by the destabilizing influence of the perturbed bootstrap current. Such modes are conventionally termed *neoclassical tearing modes*.

B. Nonlinear coupling

Equations (48), (49), (53)–(55), and (70) yield

$$\mathcal{C}^{\,n_1,n_2,n_3}_{m_1,m_2,m_3} = \frac{3\,q_a}{2}\,\frac{m_1\,m_2\,m_3}{(m_1 - n_1\,q_0)\,(m_2 - n_2\,q_0)\,(m_3 - n_3\,q_0)} \times (\bar{m} - 1 - \bar{n}\,q_0)\,\hat{\psi}^{\,m_1,n_1}(c)\,\hat{\psi}^{\,m_2,n_2}(c)\,\hat{\psi}^{\,m_3,n_3}(c), \tag{71}$$

where

$$\bar{m} = \frac{m_1 + m_2 + m_3}{3} = \frac{2m_3}{3}, \tag{72}$$

$$\bar{n} = \frac{n_1 + n_2 + n_3}{3} = \frac{2n_3}{3}. \tag{73}$$

Thus, it follows from Eq. (69) that

$$\mathcal{C}^{\,n_1,n_2,n_3}_{m_1,m_2,m_2} = \frac{3\,q_a}{2}\,(\bar{m} - 1 - \bar{n}\,q_0)\,\mathcal{A}^{\,m_1,n_1}\,\mathcal{A}^{\,m_2,n_2}\,\mathcal{A}^{\,m_3,n_3}, \tag{74}$$

where

$$\mathcal{A}^{\,m,n} = \frac{m}{(m - 1 - n\,q_0)\,(m/n\,q_0)^{\,m/2} + (n\,q_0/m)^{\,m/2}}. \tag{75}$$

It is easily demonstrated that $\mathcal{A}^{\,m,n} > 0$ provided that $n\,q_0 < m$, as must be the case for a resonant tearing mode. Moreover, $\bar{m} - 1 - \bar{n}\,q_0 > 0$ provided that

$$q_0 < \frac{m_3 - 3/2}{n_3}, \tag{76}$$

as is assumed to be the case.

C. Island width evolution equations

According to Eqs. (30), (31), (34), (45)–(47), (52), (63), and (74), the Rutherford island width evolution equations of the three coupled tearing modes take the form

$$\tau_R\,(\hat{r}^{\,m_1,n_1})^2\,\frac{dw^{\,m_1,n_1}}{dt} = E^{\,m_1,n_1} + \hat{\beta}_0\left(\frac{m_1}{n_1}\right)^2\frac{\sqrt{\hat{r}^{\,m_1,n_1}}}{w^{\,m_1,n_1}} + \frac{3}{2}\,(\bar{m} - 1 - \bar{n}\,q_0)\,\mathcal{A}^{\,m_1,n_1}\,\mathcal{A}^{\,m_2,n_2} \times \mathcal{A}^{\,m_3,n_3}\,\frac{(w^{\,m_2,n_2})^2\,(w^{\,m_3,n_3})^2}{(w^{\,m_1,n_1})^2}\,\cos\varphi, \tag{77}$$

$$\tau_R\,(\hat{r}^{\,m_2,n_2})^2\,\frac{dw^{\,m_2,n_2}}{dt} = E^{\,m_2,n_2} + \hat{\beta}_0\left(\frac{m_2}{n_2}\right)^2\frac{\sqrt{\hat{r}^{\,m_2,n_2}}}{w^{\,m_2,n_2}} + \frac{3}{2}\,(\bar{m} - 1 - \bar{n}\,q_0)\,\mathcal{A}^{\,m_1,n_1}\,\mathcal{A}^{\,m_2,n_2} \times \mathcal{A}^{\,m_3,n_3}\,\frac{(w^{\,m_1,n_1})^2\,(w^{\,m_3,n_3})^2}{(w^{\,m_2,n_2})^2}\,\cos\varphi, \tag{78}$$

$$\tau_R\,(\hat{r}^{\,m_3,n_3})^2\,\frac{dw^{\,m_3,n_3}}{dt} = E^{\,m_3,n_3} + \hat{\beta}_0\left(\frac{m_3}{n_3}\right)^2\frac{\sqrt{\hat{r}^{\,m_3,n_3}}}{w^{\,m_3,n_3}} + \frac{3}{2}\,(\bar{m} - 1 - \bar{n}\,q_0)\,\mathcal{A}^{\,m_1,n_1}\,\mathcal{A}^{\,m_2,n_2} \times \mathcal{A}^{\,m_3,n_3}\,\frac{(w^{\,m_1,n_1})^2\,(w^{\,m_2,n_2})^2}{(w^{\,m_3,n_3})^2}\,\cos\varphi, \tag{79}$$

where

$$w^{\,m,n} = \frac{W^{\,m,n}}{2^{\,3/2}\,\hat{r}^{\,m,n}}, \tag{80}$$

and

$$\varphi = \varphi^{\,m_1,n_1} + \varphi^{\,m_2,n_2} - \varphi^{\,m_3,n_3}. \tag{81}$$

Note that $\hat{\Psi}^{\,m,n} = (w^{\,m,n})^2/q_a$. Furthermore, $\tau_R = 0.8227\,(2^{\,3/2}\,\mu_0\,a^2/\eta)$ is the effective resistive evolution timescale of the plasma. Here, for the sake of simplicity, the plasma resistivity, η, is assumed to be uniform across the plasma. Finally

$$\hat{\beta}_0 = 3.27\,\frac{\beta_0}{\epsilon^{\,3/2}}, \tag{82}$$

$$\beta_0 = \frac{\mu_0 p_0}{B_\phi^2}, \tag{83}$$

where, for the sake of simplicity, the pressure profile is assumed to take the form $p(\hat{r}) = p_0\,(1-\hat{r}^{\,2})$.

D. Electromagnetic torques

Equations (30), (31), (37), (45)–(47), (52), (63), (74), and (80) imply that the normalized toroidal electromagnetic torques that develop at the three rational surfaces are

$$\delta\hat{T}_{\rm EM}^{\,m_1,n_1} = -n_1\,\delta\hat{T}_{\rm EM}, \tag{84}$$

$$\delta\hat{T}_{\rm EM}^{\,m_2,n_2} = -n_2\,\delta\hat{T}_{\rm EM}, \tag{85}$$

$$\delta\hat{T}_{\rm EM}^{\,m_3,n_3} = n_3\,\delta\hat{T}_{\rm EM}, \tag{86}$$

where

$$\delta\hat{T}_{\rm EM} = \frac{3}{2\,q_a^2}\,(\bar{m}-1-\bar{n}\,q_0)\,\mathcal{A}^{\,m_1,n_1}\,\mathcal{A}^{\,m_2,n_2}\,\mathcal{A}^{\,m_3,n_3} \times (w^{\,m_1,n_1})^{\,2}\,(w^{\,m_2,n_2})^{\,2}\,(w^{\,m_3,n_3})^{\,2}\,\sin\varphi. \tag{87}$$

E. Modified toroidal angular velocity profile

The analysis of Sec. II F reveals that

$$\tau_M\,\frac{\partial\Delta\Omega_\phi}{\partial t} - \frac{1}{\hat{r}}\,\frac{\partial}{\partial\hat{r}}\left(\hat{r}\,\frac{\partial\Delta\Omega_\phi}{\partial\hat{r}}\right) = 0, \tag{88}$$

where

$$\frac{\partial\Delta\Omega_\phi(0,t)}{\partial\hat{r}} = \Delta\Omega_\phi(1,t) = 0, \tag{89}$$

and $\Delta\Omega_\phi(\hat{r},t)$ is the modification to the plasma toroidal angular velocity profile due to the aforementioned electromagnetic torques. Here, $\tau_M = a^2\rho/\mu$ is the plasma momentum diffusion timescale. Note that, for the sake of simplicity, the plasma mass density, ρ, and viscosity, μ, are assumed to be uniform across the plasma. Finally

$$\left[\hat{r}\,\frac{\partial\Delta\Omega_\phi}{\partial\hat{r}}\right]_{\hat{r}_-^{\,m_1,n_1}}^{\hat{r}_+^{\,m_1,n_1}} = n_1\,T, \tag{90}$$

$$\left[\hat{r}\,\frac{\partial\Delta\Omega_\phi}{\partial\hat{r}}\right]_{\hat{r}_-^{\,m_2,n_2}}^{\hat{r}_+^{\,m_2,n_2}} = n_2\,T, \tag{91}$$

$$\left[\hat{r}\,\frac{\partial\Delta\Omega_\phi}{\partial\hat{r}}\right]_{\hat{r}_-^{\,m_3,n_3}}^{\hat{r}_+^{\,m_3,n_3}} = -n_3\,T, \tag{92}$$

where

$$T = \frac{3}{4}\,\frac{\epsilon^2\,\tau_M}{q_a^2\,\tau_H^2}\,(\bar{m}-1-\bar{n}\,q_0)\,\mathcal{A}^{\,m_1,n_1}\,\mathcal{A}^{\,m_2,n_2}\,\mathcal{A}^{\,m_3,n_3} \times (w^{\,m_1,n_1})^{\,2}\,(w^{\,m_2,n_2})^{\,2}\,(w^{\,m_3,n_3})^{\,2}\,\sin\varphi, \tag{93}$$

and $\tau_H = R_0\sqrt{\mu_0\,\rho}/B_\phi$ is the plasma hydromagnetic timescale. Here, use has been made of Eqs. (84)–(87).

F. Slip frequency

According to Eq. (81), we can write

$$\frac{d\varphi}{dt} = \omega, \tag{94}$$

where

$$\omega(t) = \frac{d\varphi^{\,m_1,n_1}}{dt} + \frac{d\varphi^{\,m_2,n_2}}{dt} - \frac{d\varphi^{\,m_3,n_3}}{dt}, \tag{95}$$

is the so-called *slip frequency*.[30] It follows from Eq. (35) that

$$\omega = -m_1\,\Omega_\theta^{\,m_1,n_1} - m_2\,\Omega_\theta^{\,m_2,n_2} + m_3\,\Omega_\theta^{\,m_3,n_3} + n_1\,\Omega_\phi^{\,m_1,n_1} + n_2\,\Omega_\phi^{\,m_2,n_2} - n_3\,\Omega_\phi^{\,m_3,n_3}. \tag{96}$$

Hence

$$\omega(t) = \omega_0 + n_1\,\Delta\Omega_\phi^{\,m_1,n_1}(t) + n_2\,\Delta\Omega_\phi^{\,m_2,n_2}(t) - n_3\,\Delta\Omega_\phi^{\,m_3,n_3}(t), \tag{97}$$

where ω_0 is the unperturbed slip frequency (i.e., the slip frequency in the absence of electromagnetic torques), $\Delta\Omega_\phi^{\,m_1,n_1}(t) = \Delta\Omega_\phi(\hat{r}^{\,m_1,n_1},t)$, etc.

G. Non-phase-locked state—I

Consider, first, the non-phase-locked state in which the slip frequency, ω, is non-zero.

Assuming that the slip frequency is sufficiently large [see Eq. (110)], we can neglect the terms in Eq. (77)–(79) that depend on $\cos\varphi$ (and, therefore, oscillate at the angular frequency ω), to lowest order, to give

$$w^{\,m_1,n_1}(t) \simeq \bar{w}^{\,m_1,n_1}, \tag{98}$$

$$w^{\,m_2,n_2}(t) \simeq \bar{w}^{\,m_2,n_2}, \tag{99}$$

$$w^{\,m_3,n_3}(t) \simeq \bar{w}^{\,m_3,n_3}, \tag{100}$$

where

$$\bar{w}^{\,m_1,n_1} = \hat{\beta}_0\left(\frac{m_1}{n_1}\right)^2\frac{\sqrt{\hat{r}^{\,m_1,n_1}}}{(-E^{\,m_1,n_1})}, \tag{101}$$

$$\bar{w}^{\,m_2,n_2} = \hat{\beta}_0\left(\frac{m_2}{n_2}\right)^2\frac{\sqrt{\hat{r}^{\,m_2,n_2}}}{(-E^{\,m_2,n_2})}, \tag{102}$$

$$\bar{w}^{\,m_3,n_3} = \hat{\beta}_0\left(\frac{m_3}{n_3}\right)^2\frac{\sqrt{\hat{r}^{\,m_3,n_3}}}{(-E^{\,m_3,n_3})}. \tag{103}$$

To next order, we can write

$$w^{\,m_1,n_1}(t) \simeq \bar{w}^{\,m_1,n_1} + \delta w^{\,m_1,n_1}\,\sin\varphi(t), \tag{104}$$

$$w^{\,m_2,n_2}(t) \simeq \bar{w}^{\,m_2,n_2} + \delta w^{\,m_2,n_2}\,\sin\varphi(t), \tag{105}$$

$$w^{\,m_3,n_3}(t) \simeq \bar{w}^{\,m_3,n_3} + \delta w^{\,m_3,n_3}\,\sin\varphi(t), \tag{106}$$

where $\delta w^{\,m_1,n_1}/\bar{w}^{\,m_1,n_1} \ll 1$, etc. It follows from Eqs. (77)–(79) and (94) that

$$\delta w^{\,m_1,n_1} = \frac{3}{2}\,\frac{1}{\omega\,\tau_R}\,(\bar{m}-1-\bar{n}\,q_0)\,\mathcal{A}^{\,m_1,n_1}\,\mathcal{A}^{\,m_2,n_2}\,\mathcal{A}^{\,m_3,n_3} \times \frac{(\bar{w}^{\,m_2,n_2})^{\,2}\,(\bar{w}^{\,m_3,n_3})^{\,2}}{(\hat{r}^{\,m_1,n_1})^{\,2}\,(\bar{w}^{\,m_1,n_1})^{\,2}}, \tag{107}$$

$$\delta w^{m_2,n_2} = \frac{3}{2}\frac{1}{\omega\,\tau_R}\,(\bar{m}-1-\bar{n}\,q_0)\,\mathcal{A}^{m_1,n_1}\,\mathcal{A}^{m_2,,n_2}\,\mathcal{A}^{m_3,n_3} \times \frac{(\bar{w}^{\,m_1,n_1})^{\,2}\,(\bar{w}^{\,m_3,n_3})^{\,2}}{(\hat{r}^{\,m_2,n_2})^{\,2}\,(\bar{w}^{\,m_2,n_2})^{\,2}}, \tag{108}$$

$$\delta w^{m_3,n_3} = \frac{3}{2}\frac{1}{\omega\,\tau_R}\,(\bar{m}-1-\bar{n}\,q_0)\,\mathcal{A}^{m_1,n_1}\,\mathcal{A}^{m_2,n_2}\,\mathcal{A}^{m_3,n_3} \times \frac{(\bar{w}^{\,m_1,n_1})^{\,2}\,(\bar{w}^{\,m_2,n_2})^{\,2}}{(\hat{r}^{\,m_3,n_3})^{\,2}\,(\bar{w}^{\,m_3,n_3})^{\,2}}. \tag{109}$$

The constraints $\delta w^{m_1,n_1}/\bar{w}^{\,m_1,n_1} \ll 1$, etc., imply that

$$\omega\,\tau_R \gg \frac{3}{2}\,(\bar{m}-1-\bar{n}\,q_0)\,\mathcal{A}^{m_1,n_1}\,\mathcal{A}^{m_2,n_2}\,\mathcal{A}^{m_3,n_3} \times \frac{(\bar{w}^{\,m_2,n_2})^{\,2}\,(\bar{w}^{\,m_3,n_3})^{\,2}}{(\hat{r}^{\,m_1,n_1})^{\,2}\,(\bar{w}^{\,m_1,n_1})^{\,3}}, \tag{110}$$

etc. In other words, Eqs. (104)–(106) are valid provided that the slip frequency is sufficiently large.

To first order in small quantities, Eqs. (93) and (104)–(106) yield

$$T(t) \simeq T_0\,\sin\varphi(t) + 2\,\delta T\,\sin^2\varphi(t), \tag{111}$$

where

$$T_0 = \frac{3}{4}\frac{\epsilon^{\,2}\,\tau_M}{q_a^{\,2}\,\tau_H^{\,2}}\,(\bar{m}-1-\bar{n}\,q_0)\,\mathcal{A}^{m_1,n_1}\,\mathcal{A}^{m_2,n_2}\,\mathcal{A}^{m_3,n_3} \times (\bar{w}^{\,m_1,n_1})^{\,2}\,(\bar{w}^{\,m_2,n_2})^{\,2}\,(\bar{w}^{\,m_3,n_3})^{\,2}, \tag{112}$$

and

$$\delta T = \frac{3}{4}\frac{\epsilon^{\,2}\,\tau_M}{q_a^{\,2}\,\tau_H^{\,2}}\,(\bar{m}-1-\bar{n}\,q_0)\,\mathcal{A}^{m_1,n_1}\,\mathcal{A}^{m_2,n_2}\,\mathcal{A}^{m_3,n_3} \times (\bar{w}^{\,m_1,n_1})^{\,2}\,(\bar{w}^{\,m_2,n_2})^{\,2}\,(\bar{w}^{\,m_3,n_3})^{\,2} \times \left(\frac{\delta w^{m_1,m_1}}{\bar{w}^{\,m_1,n_1}} + \frac{\delta w^{m_2,m_2}}{\bar{w}^{\,m_2,n_2}} + \frac{\delta w^{m_2,m_2}}{\bar{w}^{\,m_2,n_2}}\right), \tag{113}$$

or, making use of Eqs. (107)–(109)

$$\delta T = \frac{3^{\,2}}{2^{\,3}}\frac{\epsilon^{\,2}}{q_a^{\,2}}\frac{\tau_M}{\omega\,\tau_R\,\tau_H^{\,2}}\,(\bar{m}-1-\bar{n}\,q_0)^{\,2}(\mathcal{A}^{m_1,n_1}\,\mathcal{A}^{m_2,n_2}\,\mathcal{A}^{m_3,n_3})^2 \times \left[\frac{(\bar{w}^{\,m_2,n_2})^{\,4}\,(\bar{w}^{\,m_3,n_3})^{\,4}}{(\hat{r}^{\,m_1,n_1})^{\,2}\,\bar{w}^{\,m_1,n_1}} + \frac{(\bar{w}^{\,m_1,n_1})^{\,4}\,(\bar{w}^{\,m_3,n_3})^{\,4}}{(\hat{r}^{\,m_2,n_2})^{\,2}\,\bar{w}^{\,m_2,n_2}} + \frac{(\bar{w}^{\,m_1,n_1})^{\,4}\,(\bar{w}^{\,m_2,n_2})^{\,4}}{(\hat{r}^{\,m_3,n_3})^{\,2}\,\bar{w}^{\,m_3,n_3}}\right]. \tag{114}$$

Let us assume that the plasma toroidal rotation profile only responds appreciably to the *time-averaged* component of the electromagnetic torque

$$\langle T\rangle = \delta T, \tag{115}$$

which turns out to be the case provided that τ_M is sufficiently large [see Eq. (160)]. It thus follows that $\Delta\Omega_\phi(\hat{r},t) = \Delta\Omega_\phi(\hat{r})$. Hence, from Eqs. (88)–(92)

$$\frac{d}{d\hat{r}}\left(\hat{r}\,\frac{d\Delta\Omega_\phi}{d\hat{r}}\right) = 0, \tag{116}$$

where

$$\frac{d\Delta\Omega_\phi(0)}{d\hat{r}} = \Delta\Omega_\phi(1) = 0, \tag{117}$$

and

$$\left[\hat{r}\,\frac{d\Delta\Omega_\phi}{d\hat{r}}\right]_{\hat{r}_-^{\,m_1,n_1}}^{\hat{r}_+^{\,m_1,n_1}} = n_1\,\delta T, \tag{118}$$

$$\left[\hat{r}\,\frac{d\Delta\Omega_\phi}{d\hat{r}}\right]_{\hat{r}_-^{\,m_2,n_2}}^{\hat{r}_+^{\,m_2,n_2}} = n_2\,\delta T, \tag{119}$$

$$\left[\hat{r}\,\frac{d\Delta\Omega_\phi}{d\hat{r}}\right]_{\hat{r}_-^{\,m_3,n_3}}^{\hat{r}_+^{\,m_3,n_3}} = -n_3\,\delta T. \tag{120}$$

The solution of Eqs. (116)–(120) is

$$\Delta\Omega_\phi(\hat{r}) = \Delta\Omega_\phi^{\,m_1,n_1}, \tag{121}$$

for $0 \le \hat{r} \le \hat{r}^{\,m_1,n_1}$, and

$$\Delta\Omega_\phi(\hat{r}) = \Delta\Omega_\phi^{\,m_3,n_3} + \left(\Delta\Omega_\phi^{\,m_1,n_1} - \Delta\Omega_\phi^{\,m_3,n_3}\right) \times \frac{\ln(\hat{r}/\hat{r}^{\,m_3,n_3})}{\ln(\hat{r}^{\,m_1,n_1}/\hat{r}^{\,m_3,n_3})}, \tag{122}$$

for $\hat{r}^{\,m_1,n_1} < \hat{r} \le \hat{r}^{\,m_3,n_3}$, and

$$\Delta\Omega_\phi(\hat{r}) = \Delta\Omega_\phi^{\,m_3,n_3}\,\frac{\ln(\hat{r}/\hat{r}^{\,m_2,n_2})}{\ln(\hat{r}^{\,m_3,n_3}/\hat{r}^{\,m_2,n_2})}, \tag{123}$$

for $\hat{r}^{\,m_3,n_3} < \hat{r} \le \hat{r}^{\,m_2,n_2}$, and

$$\Delta\Omega_\phi(\hat{r}) = 0, \tag{124}$$

for $\hat{r} > \hat{r}^{\,m_2,n_2}$, where

$$\Delta\Omega_\phi^{\,m_1,n_1} = \Delta\Omega_\phi^{\,m_3,n_3} - n_1\,\ln\left(\frac{\hat{r}^{\,m_3,n_3}}{\hat{r}^{\,m_1,n_1}}\right)\delta T, \tag{125}$$

$$\Delta\Omega_\phi^{\,m_2,n_2} = 0, \tag{126}$$

$$\Delta\Omega_\phi^{\,m_3,n_3} = n_2\,\ln\left(\frac{\hat{r}^{\,m_2,n_2}}{\hat{r}^{\,m_3,n_3}}\right)\delta T, \tag{127}$$

which implies, from Eq. (97), that

$$\omega = \omega_0 - \left[n_1^{\,2}\,\ln\left(\frac{\hat{r}^{\,m_3,n_3}}{\hat{r}^{\,m_1,n_1}}\right) + n_2^{\,2}\,\ln\left(\frac{\hat{r}^{\,m_2,n_2}}{\hat{r}^{\,m_3,n_3}}\right)\right]\delta T. \tag{128}$$

Note that the modification to the plasma toroidal angular velocity profile is localized to the region of the plasma lying within the outermost coupled rational surface.

Combining Eqs. (114) and (128), we obtain the torque balance equation

$$4\,(1-\hat{\omega})\,\hat{\omega} = F, \tag{129}$$

where $\hat{\omega} = \omega/\omega_0$, and

$$F = \frac{3^2}{2}\,\frac{\epsilon^2}{q_a^2}\,\frac{\tau_M}{\tau_R\,(\omega_0\,\tau_H)^2}\left[n_1^2\,\ln\left(\frac{\hat{r}^{\,m_3,n_3}}{\hat{r}^{\,m_1,n_1}}\right)+n_2^2\,\ln\left(\frac{\hat{r}^{\,m_2,n_2}}{\hat{r}^{\,m_3,n_3}}\right)\right]$$
$$\times\,(\bar{m}-1-\bar{n}\,q_0)^2\,(\mathcal{A}^{m_1,n_1}\,\mathcal{A}^{m_2,n_2}\,\mathcal{A}^{m_3,n_3})^2\,\mathcal{W}, \tag{130}$$

with

$$\mathcal{W} = \frac{(\bar{w}^{\,m_2,n_2})^4\,(\bar{w}^{m_3,n_3})^4}{(\hat{r}^{\,m_1,n_1})^{\,2}\,\bar{w}^{\,m_1,n_1}}+\frac{(\bar{w}^{\,m_1,n_1})^4\,(\bar{w}^{m_3,n_3})^4}{(\hat{r}^{\,m_2,n_2})^{\,2}\,\bar{w}^{\,m_2,n_2}}$$
$$+\frac{(\bar{w}^{\,m_1,n_1})^4\,(\bar{w}^{m_2,n_2})^4}{(\hat{r}^{\,m_3,n_3})^{\,2}\,\bar{w}^{\,m_3,n_3}}. \tag{131}$$

For $0 \leq F < 1$, the torque balance equation, (129), possesses two solutions. One, which is characterized by $1/2 < \hat{\omega} \leq 0$, is dynamically stable, whereas the other is dynamically unstable.[30] When F reaches the critical amplitude unity, at which point the slip frequency has been reduced to one half of its unperturbed value, the stable and unstable solutions annihilate, and there is a bifurcation to a phase-locked state.[30,32]

Incidentally, it is clear, from the previous discussion, that there is considerable overlap between the theory of the nonlinear mode coupling of three rotating tearing modes in a tokamak plasma and that of the locking of a single rotating tearing mode to a resonant error-field.[30,32] In the former case, two tearing modes in the triplet beat together to form an effective error-field that acts to phase lock the third mode. The amplitude of the effective error-field is proportional to the product of the amplitudes of the two beating modes, whereas its rotation frequency is either the sum or the difference of the rotation frequencies of the beating modes.

H. Non-phase-locked state—II

In Sec. IV G, we simplified our calculation by assuming that the plasma toroidal rotation profile only responds appreciably to the time-averaged component of the electromagnetic torques that develop at the three coupled rational surfaces. Let us now consider the response of the rotation profile to the much larger amplitude time-varying components of these torques. According to Eq. (111), we have

$$T(t) \simeq T_0\,\sin\varphi(t) + \delta T, \tag{132}$$

where we have only retained the time-averaged component of the first-order term. Let us write

$$\Delta\Omega_\phi(\hat{r},t) = \Delta\Omega_\phi^0(\hat{r}) + \Delta\Omega_\phi^c(\hat{r})\,\cos\varphi(t) + \Delta\Omega_\phi^s(\hat{r})\,\sin\varphi(t). \tag{133}$$

It follows from Eqs. (88)–(92) that $\Delta\Omega_\phi^0$ satisfies Eqs. (116)–(120). Furthermore, because $\omega = d\varphi/dt$

$$\frac{1}{\hat{r}}\,\frac{d}{d\hat{r}}\left(\hat{r}\,\frac{d\Delta\Omega_\phi^c}{d\hat{r}}\right) = \omega\,\tau_M\,\Delta\Omega_\phi^s, \tag{134}$$

$$\frac{1}{\hat{r}}\,\frac{d}{d\hat{r}}\left(\hat{r}\,\frac{d\Delta\Omega_\phi^s}{d\hat{r}}\right) = -\omega\,\tau_M\,\Delta\Omega_\phi^c, \tag{135}$$

where

$$\frac{d\Delta\Omega_\phi^{c,s}(0)}{d\hat{r}} = \Delta\Omega_\phi^{c,s}(1) = 0, \tag{136}$$

and

$$\left[\hat{r}\,\frac{d\Delta\Omega_\phi^c}{d\hat{r}}\right]_{\hat{r}_-^{\,m_1,n_1}}^{\hat{r}_+^{\,m_1,n_1}} = \left[\hat{r}\,\frac{d\Delta\Omega_\phi^c}{d\hat{r}}\right]_{\hat{r}_-^{\,m_2,n_2}}^{\hat{r}_+^{\,m_2,n_2}} = \left[\hat{r}\,\frac{d\Delta\Omega_\phi^c}{d\hat{r}}\right]_{\hat{r}_-^{\,m_3,n_3}}^{\hat{r}_+^{\,m_3,n_3}} = 0. \tag{137}$$

Finally

$$\left[\hat{r}\,\frac{d\Delta\Omega_\phi^s}{d\hat{r}}\right]_{\hat{r}_-^{\,m_1,n_1}}^{\hat{r}_+^{\,m_1,n_1}} = n_1\,T_0, \tag{138}$$

$$\left[\hat{r}\,\frac{d\Delta\Omega_\phi^s}{d\hat{r}}\right]_{\hat{r}_-^{\,m_2,n_2}}^{\hat{r}_+^{\,m_2,n_2}} = n_2\,T_0, \tag{139}$$

$$\left[\hat{r}\,\frac{d\Delta\Omega_\phi^s}{d\hat{r}}\right]_{\hat{r}_-^{\,m_3,n_3}}^{\hat{r}_+^{\,m_3,n_3}} = -n_3\,T_0. \tag{140}$$

In the limit $\omega\,\tau_M \gg 1$, the solution of Eqs. (134)–(140) is such that

$$\Delta\Omega_\phi^c(\hat{r}^{\,m_1,n_1}) = -\Delta\Omega_\phi^s(\hat{r}^{\,m_1,n_1}) \simeq \frac{n_1\,T_0}{\hat{r}^{\,m_1,n_1}\,\sqrt{8\,\omega\,\tau_M}}, \tag{141}$$

$$\Delta\Omega_\phi^c(\hat{r}^{\,m_2,n_2}) = -\Delta\Omega_\phi^s(\hat{r}^{\,m_2,n_2}) \simeq \frac{n_2\,T_0}{\hat{r}^{\,m_2,n_2}\,\sqrt{8\,\omega\,\tau_M}}, \tag{142}$$

$$\Delta\Omega_\phi^c(\hat{r}^{\,m_3,n_3}) = -\Delta\Omega_\phi^s(\hat{r}^{\,m_3,n_3}) \simeq -\frac{n_3\,T_0}{\hat{r}^{\,m_3,n_3}\,\sqrt{8\,\omega\,\tau_M}}. \tag{143}$$

Thus, it follows from Eqs. (97) and (133) that

$$\omega(t) = \omega_0 - \left[n_1^2\,\ln\left(\frac{\hat{r}^{\,m_3,n_3}}{\hat{r}^{\,m_1,n_1}}\right)+n_2^2\,\ln\left(\frac{\hat{r}^{\,m_2,n_2}}{\hat{r}^{\,m_3,n_3}}\right)\right]\delta T$$
$$+\left(\frac{n_1^2}{\hat{r}^{\,m_1,n_1}}+\frac{n_2^2}{\hat{r}^{\,m_2,n_2}}+\frac{n_3^2}{\hat{r}^{\,m_3,n_3}}\right)$$
$$\times\,\frac{T_0}{\sqrt{8\,\omega\,\tau_M}}\,(\cos\varphi-\sin\varphi), \tag{144}$$

where use has been made of Eq. (128). It can be seen that the time-varying components of the electromagnetic torques that develop at the three coupled rational surfaces give rise to a modulation of the slip frequency. Given that $\omega = d\varphi/dt$, we can integrate the previous equation to give

$$\varphi(t) = \bar{\varphi}(t) + \left(\frac{n_1^2}{\hat{r}^{\,m_1,n_1}}+\frac{n_2^2}{\hat{r}^{\,m_2,n_2}}+\frac{n_3^2}{\hat{r}^{\,m_3,n_3}}\right)$$
$$\times\,\frac{T_0}{\bar{\omega}\sqrt{8\,\bar{\omega}\,\tau_M}}\,(\sin\bar{\varphi}+\cos\bar{\varphi}), \tag{145}$$

where

$$\frac{d\bar{\varphi}}{dt} = \bar{\omega}, \tag{146}$$

and

$$\bar{\omega} = \omega_0 - \left[n_1^2\,\ln\left(\frac{\hat{r}^{\,m_3,n_3}}{\hat{r}^{\,m_1,n_1}}\right)+n_2^2\,\ln\left(\frac{\hat{r}^{\,m_2,n_2}}{\hat{r}^{\,m_3,n_3}}\right)\right]\delta T, \tag{147}$$

is the steady-state slip frequency.

The time-averaged component of the Rutherford island width evolution equation, (77), can be rearranged to give

$$1-\frac{\bar{w}^{\,m_1,n_1}}{w^{\,m_1,n_1}}=\frac{3}{2}\,(\bar{m}-1-\bar{n}\,q_0)\,\mathcal{A}^{\,m_1,n_1}\,\mathcal{A}^{\,m_2,n_2}\,\mathcal{A}^{\,m_3,n_3}\times\frac{(\bar{w}^{\,m_2,n_2})^{\,2}\,(\bar{w}^{\,m_3,n_3})^{\,2}}{(-E^{\,m_1,n_1})\,(\bar{w}^{\,m_1,n_1})^{\,2}}\,\langle\cos\varphi\rangle,\tag{148}$$

where $\bar{w}^{\,m_1,n_1}$ is specified in Eq. (101). However, according to Eq. (145)

$$\cos\varphi\simeq\cos\bar{\varphi}-\sin\bar{\varphi}\left(\frac{n_1^2}{\hat{r}^{\,m_1,n_1}}+\frac{n_2^2}{\hat{r}^{\,m_2,n_2}}+\frac{n_3^2}{\hat{r}^{\,m_3,n_3}}\right)\times\frac{T_0}{\bar{\omega}\sqrt{8\,\bar{\omega}\,\tau_M}}\,(\sin\bar{\varphi}+\cos\bar{\varphi}).\tag{149}$$

Hence

$$\langle\cos\phi\rangle\simeq-\left(\frac{n_1^2}{\hat{r}^{\,m_1,n_1}}+\frac{n_2^2}{\hat{r}^{\,m_2,n_2}}+\frac{n_3^2}{\hat{r}^{\,m_3,n_3}}\right)\frac{T_0}{\bar{\omega}\sqrt{32\,\bar{\omega}\,\tau_M}}.\tag{150}$$

Equation (148) then yields

$$w^{\,m_1,n_1}(t)=\bar{w}^{\,m_1,n_1}-\delta\bar{w}^{\,m_1,n_1},\tag{151}$$

where

$$\frac{\delta\bar{w}^{\,m_1,n_1}}{\bar{w}^{\,m_1,n_1}}=\frac{3}{2}\,(\bar{m}-1-\bar{n}\,q_0)\,\mathcal{A}^{\,m_1,n_1}\,\mathcal{A}^{\,m_2,n_2}\,\mathcal{A}^{\,m_3,n_3}\times\frac{(\bar{w}^{\,m_2,n_2})^{\,2}\,(\bar{w}^{\,m_3,n_3})^{\,2}}{(-E^{\,m_1,n_1})\,(\bar{w}^{\,m_1,n_1})^{\,2}}\times\left(\frac{n_1^2}{\hat{r}^{\,m_1,n_1}}+\frac{n_2^2}{\hat{r}^{\,m_2,n_2}}+\frac{n_3^2}{\hat{r}^{\,m_3,n_3}}\right)\frac{T_0}{\sqrt{32\,\bar{\omega}\,\tau_M}\,\bar{\omega}}.\tag{152}$$

If we now take time variation into account in the Rutherford equation, as described in Sec. IV G, then we obtain

$$w^{\,m_1,n_1}(t)=\bar{w}^{\,m_1,n_1}-\delta\bar{w}^{\,m_1,n_1}+\delta w^{\,m_1,n_1}\,\sin\bar{\varphi}(t),\tag{153}$$

where $\delta w^{\,m_1,n_1}$ is specified in Eq. (107) (with ω replaced by $\bar{\omega}$). We can perform similar analysis for the Rutherford equations (78) and (79).

Thus, taking the time-varying, as well as the steady-state, components of the electromagnetic torques acting at the three coupled rational surfaces into account in our analysis; we deduce that the normalized island widths vary as

$$w^{\,m_1,n_1}(t)=\bar{w}^{\,m_1,n_1}-\delta\bar{w}^{\,m_1,n_1}+\delta w^{\,m_1,n_1}\,\sin\bar{\varphi}(t),\tag{154}$$

$$w^{\,m_2,n_2}(t)=\bar{w}^{\,m_2,n_2}-\delta\bar{w}^{\,m_2,n_2}+\delta w^{\,m_2,n_2}\,\sin\bar{\varphi}(t),\tag{155}$$

$$w^{\,m_3,n_3}(t)=\bar{w}^{\,m_3,n_3}-\delta\bar{w}^{\,m_3,n_3}+\delta w^{\,m_3,n_3}\,\sin\bar{\varphi}(t),\tag{156}$$

where $\bar{w}^{\,m_1,n_1}$, $\bar{w}^{\,m_1,n_1}$, and $\bar{w}^{\,m_3,n_3}$ are specified in Eqs. (101)–(103), whereas $\delta w^{\,m_1,n_1}$, $\delta w^{\,m_2,n_2}$, and $\delta w^{\,m_3,n_3}$ are given by Eqs. (107)–(109) (with ω replaced by $\bar{\omega}$). Here, $\bar{\varphi}$ and $\bar{\omega}$ are defined in Eqs. (146) and (147), respectively. Finally

$$\frac{\delta\bar{w}^{\,m_1,n_1}}{\bar{w}^{\,m_1,n_1}}=\frac{3^2}{2}\,\frac{\epsilon^2}{q_a^2}\,\frac{\tau_M}{\tau_R\,(\bar{\omega}\,\tau_H)^{\,2}}\,\frac{\bar{\omega}\,\tau_R}{(512\,\bar{\omega}\,\tau_M)^{\,1/2}}\times\left(\frac{n_1^2}{\hat{r}^{\,m_1,n_1}}+\frac{n_2^2}{\hat{r}^{\,m_2,n_2}}+\frac{n_3^2}{\hat{r}^{\,m_3,n_3}}\right)\times(\bar{m}-1-\bar{n}\,q_0)^2\,(\mathcal{A}^{\,m_1,n_1}\,\mathcal{A}^{\,m_2,n_2}\,\mathcal{A}^{\,m_3,n_3})^{\,2}\times\frac{(\bar{w}^{\,m_2,n_2})^{\,4}\,(\bar{w}^{\,m_3,n_3})^{\,4}}{(-E^{\,m_1,n_1})},\tag{157}$$

$$\frac{\delta\bar{w}^{\,m_2,n_2}}{\bar{w}^{\,m_2,n_2}}=\frac{3^2}{2}\,\frac{\epsilon^2}{q_a^2}\,\frac{\tau_M}{\tau_R\,(\bar{\omega}\,\tau_H)^{\,2}}\,\frac{\bar{\omega}\,\tau_R}{(512\,\bar{\omega}\,\tau_M)^{\,1/2}}\times\left(\frac{n_1^2}{\hat{r}^{\,m_1,n_1}}+\frac{n_2^2}{\hat{r}^{\,m_2,n_2}}+\frac{n_3^2}{\hat{r}^{\,m_3,n_3}}\right)(\bar{m}-1-\bar{n}\,q_0)^2\times(\mathcal{A}^{\,m_1,n_1}\,\mathcal{A}^{\,m_2,n_2}\,\mathcal{A}^{\,m_3,n_3})^{\,2}\,\frac{(\bar{w}^{\,m_1,n_1})^{\,4}\,(\bar{w}^{\,m_3,n_3})^{\,4}}{(-E^{\,m_2,n_2})},\tag{158}$$

$$\frac{\delta\bar{w}^{\,m_3,n_3}}{\bar{w}^{\,m_3,n_3}}=\frac{3^2}{2}\,\frac{\epsilon^2}{q_a^2}\,\frac{\tau_M}{\tau_R\,(\bar{\omega}\,\tau_H)^{\,2}}\,\frac{\bar{\omega}\,\tau_R}{(512\,\bar{\omega}\,\tau_M)^{\,1/2}}\times\left(\frac{n_1^2}{\hat{r}^{\,m_1,n_1}}+\frac{n_2^2}{\hat{r}^{\,m_2,n_2}}+\frac{n_3^2}{\hat{r}^{\,m_3,n_3}}\right)(\bar{m}-1-\bar{n}\,q_0)^2\times(\mathcal{A}^{\,m_1,n_1}\,\mathcal{A}^{\,m_2,n_2}\,\mathcal{A}^{\,m_3,n_3})^{\,2}\,\frac{(\bar{w}^{\,m_1,n_1})^{\,4}\,(\bar{w}^{\,m_2,n_2})^{\,4}}{(-E^{\,m_3,n_3})},\tag{159}$$

where use has been made of Eq. (112). It can be seen, from Eqs. (154)–(156), that the time-varying components of the torques act to reduce the steady-state island widths of the three coupled tearing modes (i.e., $\bar{w}^{\,m_1,n_1}\rightarrow\bar{w}^{\,m_1,n_1}-\delta\bar{w}^{\,m_1,n_1}$). The origin of this effect is the previously mentioned modulation in the slip frequency, which causes the three coupled modes to spend slightly more time in mutually stabilizing phase relations than in mutually destabilizing relations.[30] We can safely neglect this average mutual stabilization effect provided that $\delta\bar{w}^{\,m_1,n_1}/\bar{w}^{\,m_1,n_1}\ll 1$, etc., when the bifurcation to the phase-locked state, described in Sec. IV G, occurs. The bifurcation occurs when $F=1$, where F is specified in Eq. (130). Thus, a comparison of Eq. (130) and the previous three equations reveals that the neglect of the average mutual stabilization effect in the non-phase-locked state is valid provided that

$$\tau_M\gg\frac{\omega_0\,(\tau_R\,\bar{w})^2}{512},\tag{160}$$

where $\bar{w}$ is the typical value of $\bar{w}^{\,m_1,n_1}$, $\bar{w}^{\,m_2,n_2}$, and $\bar{w}^{\,m_3,n_3}$. In the following, for the sake of simplicity, we shall assume that the previous inequality is satisfied (i.e., we shall neglect $\delta\bar{w}^{\,m_1,n_1}$, $\delta\bar{w}^{\,m_2,n_2}$, and $\delta\bar{w}^{\,m_3,n_3}$).

I. Phase-locked state

The phase-locked state is characterized by zero slip frequency, i.e., $\omega=0$.[30,32] Thus, it follows from Eq. (94) that

$$\varphi(t) = \varphi_0, \tag{161}$$

where φ_0 is a constant, and from Eq. (97) that

$$0 = \omega_0 + n_1\,\Delta\Omega_\phi^{m_1,n_1} + n_2\,\Delta\Omega_\phi^{m_2,n_2} - n_3\,\Delta\Omega_\phi^{m_3,n_3}. \tag{162}$$

In the phase-locked state, we expect $\Delta\Omega_\phi(\hat{r},t) = \Delta\Omega_\phi(\hat{r})$. Thus, the modified plasma toroidal angular velocity profile is governed by Eqs. (116) and (117), where

$$\left[\hat{r}\,\frac{d\Delta\Omega_\phi}{d\hat{r}}\right]_{\hat{r}_-^{m_1,n_1}}^{\hat{r}_+^{m_1,n_1}} = n_1\,T_0, \tag{163}$$

$$\left[\hat{r}\,\frac{d\Delta\Omega_\phi}{d\hat{r}}\right]_{\hat{r}_-^{m_2,n_2}}^{\hat{r}_+^{m_2,n_2}} = n_2\,T_0, \tag{164}$$

$$\left[\hat{r}\,\frac{d\Delta\Omega_\phi}{d\hat{r}}\right]_{\hat{r}_-^{m_3,n_3}}^{\hat{r}_+^{m_3,n_3}} = -n_3\,T_0, \tag{165}$$

and

$$T_0 = \frac{3}{4}\,\frac{\epsilon^2\,\tau_M}{q_a^2\,\tau_H^2}\,(\bar{m} - 1 - \bar{n}\,q_0)\,\mathcal{A}^{m_1,n_1}\,\mathcal{A}^{m_2,n_2} \times \mathcal{A}^{m_3,n_3}\,(\bar{w}^{\,m_1,n_1})^2\,(\bar{w}^{\,m_2,n_2})^2\,(\bar{w}^{\,m_3,n_3})^2\,\sin\varphi_0. \tag{166}$$

Here, use has been made of Eqs. (90)–(93). The solution of Eqs. (116), (117), and (163)–(166) is specified by Eqs. (121)–(124), where

$$\Delta\Omega_\phi^{m_1,n_1} = \Delta\Omega_\phi^{m_3,n_3} - n_1\,\ln\left(\frac{\hat{r}^{\,m_3,n_3}}{\hat{r}^{\,m_1,n_1}}\right)T_0, \tag{167}$$

$$\Delta\Omega_\phi^{m_2,n_2} = 0, \tag{168}$$

$$\Delta\Omega_\phi^{m_3,n_3} = n_2\,\ln\left(\frac{\hat{r}^{\,m_2,n_2}}{\hat{r}^{\,m_3,n_3}}\right)T_0. \tag{169}$$

Thus, it follows from Eqs. (130), (162), and (166) that

$$\frac{\Delta\Omega_\phi^{m_1,n_1}}{\omega_0} = \frac{n_2\,\ln(\hat{r}^{\,m_2,n_2}/\hat{r}^{\,m_3,n_3})}{n_1^2\,\ln(\hat{r}^{\,m_3,n_3}/\hat{r}^{\,m_1,n_1}) + n_2^2\,\ln(\hat{r}^{\,m_2,n_2}/\hat{r}^{\,m_3,n_3})} - \frac{n_1\,\ln(\hat{r}^{\,m_3,n_3}/\hat{r}^{\,m_1,n_1})}{n_1^2\,\ln(\hat{r}^{\,m_3,n_3}/\hat{r}^{\,m_1,n_1}) + n_2^2\,\ln(\hat{r}^{\,m_2,n_2}/\hat{r}^{\,m_3,n_3})}, \tag{170}$$

$$\frac{\Delta\Omega_\phi^{m_2,n_2}}{\omega_0} = 0, \tag{171}$$

$$\frac{\Delta\Omega_\phi^{m_3,n_3}}{\omega_0} = \frac{n_2\,\ln(\hat{r}^{\,m_2,n_2}/\hat{r}^{\,m_3,n_3})}{n_1^2\,\ln(\hat{r}^{\,m_3,n_3}/\hat{r}^{\,m_1,n_1}) + n_2^2\,\ln(\hat{r}^{\,m_2,n_2}/\hat{r}^{\,m_3,n_3})}, \tag{172}$$

and

$$\sin\varphi_0 = \frac{4\,G}{F}, \tag{173}$$

where

$$G = \frac{3}{2}\,\frac{1}{\omega_0\,\tau_R}\,(\bar{m} - 1 - \bar{n}\,q_0)\,\mathcal{A}^{m_1,n_1}\,\mathcal{A}^{m_2,n_2}\,\mathcal{A}^{m_3,n_3} \times \left[\frac{(\bar{w}^{\,m_2,n_2})^2\,(\bar{w}^{\,m_3,n_3})^2}{(\hat{r}^{\,m_1,n_1})^2\,(\bar{w}^{\,m_1,n_1})^3} + \frac{(\bar{w}^{\,m_1,n_1})^2\,(\bar{w}^{\,m_3,n_3})^2}{(\hat{r}^{\,m_2,n_2})^2\,(\bar{w}^{\,m_2,n_2})^3} + \frac{(\bar{w}^{\,m_1,n_1})^2\,(\bar{w}^{\,m_2,n_2})^2}{(\hat{r}^{\,m_3,n_3})^2\,(\bar{w}^{\,m_3,n_3})^3}\right]. \tag{174}$$

Now, we know that $F \geq 1$ in the phase-locked state. Moreover, Eq. (110) implies that $G \ll 1$. Hence, Eq. (173) yields

$$\sin\varphi_0 \simeq 0. \tag{175}$$

There are two possible solutions to this equation. The first

$$\varphi_0 \simeq 0, \tag{176}$$

is dynamically stable (because the electromagnetic torques that develop at the three coupled rational surfaces have the same signs as the corresponding torques in the non-phase-locked state, and are, therefore, acting to maintain the phase locking), the second, $\varphi_0 = \pi$, is dynamically unstable.

According to Eqs. (77)–(79), (161), and (176), the Rutherford island width evolution equations of the three coupled modes in the phase-locked state take the form

$$\tau_R\,(\hat{r}^{\,m_1,n_1})^2\,\frac{dw^{m_1,n_1}}{dt} \simeq E^{m_1,n_1} + \hat{\beta}_0\left(\frac{m_1}{n_1}\right)^2\frac{\sqrt{\hat{r}^{\,m_1,n_1}}}{w^{m_1,n_1}} + \frac{3}{2}\,(\bar{m} - 1 - \bar{n}\,q_0)\,\mathcal{A}^{m_1,n_1} \times \mathcal{A}^{m_2,n_2}\,\mathcal{A}^{m_3,n_3}\,\frac{(w^{m_2,n_2})^2\,(w^{m_3,n_3})^2}{(w^{m_1,n_1})^2}, \tag{177}$$

$$\tau_R\,(\hat{r}^{\,m_2,n_2})^2\,\frac{dw^{m_2,n_2}}{dt} \simeq E^{m_2,n_2} + \hat{\beta}_0\left(\frac{m_2}{n_2}\right)^2\frac{\sqrt{\hat{r}^{\,m_2,n_2}}}{w^{m_2,n_2}} + \frac{3}{2}\,(\bar{m} - 1 - \bar{n}\,q_0)\,\mathcal{A}^{m_1,n_1} \times \mathcal{A}^{m_2,n_2}\,\mathcal{A}^{m_3,n_3}\,\frac{(w^{m_1,n_1})^2\,(w^{m_3,n_3})^2}{(w^{m_2,n_2})^2}, \tag{178}$$

$$\tau_R\,(\hat{r}^{\,m_3,n_3})^2\,\frac{dw^{m_3,n_3}}{dt} \simeq E^{m_3,n_3} + \hat{\beta}_0\left(\frac{m_3}{n_3}\right)^2\frac{\sqrt{\hat{r}^{\,m_3,n_3}}}{w^{m_3,n_3}} + \frac{3}{2}\,(\bar{m} - 1 - \bar{n}\,q_0)\,\mathcal{A}^{m_1,n_1} \times \mathcal{A}^{m_2,n_2}\,\mathcal{A}^{m_3,n_3}\,\frac{(w^{m_1,n_1})^2\,(w^{m_2,n_2})^2}{(w^{m_3,n_3})^2}. \tag{179}$$

Thus, writing

$$w^{m_1,n_1}(t) \simeq \bar{w}^{\,m_1,n_1} + \delta w^{m_1,n_1}, \tag{180}$$

$$w^{m_2,n_2}(t) \simeq \bar{w}^{\,m_2,n_2} + \delta w^{m_2,n_2}, \tag{181}$$

$$w^{m_3,n_3}(t) \simeq \bar{w}^{\,m_3,n_3} + \delta w^{m_3,n_3}, \tag{182}$$

we obtain

$$\delta w^{m_1,n_1} = \frac{3}{2}\,(\bar{m} - 1 - \bar{n}\,q_0)\,\mathcal{A}^{m_1,n_1}\,\mathcal{A}^{m_2,n_2}\,\mathcal{A}^{m_3,n_3} \times \frac{(\bar{w}^{m_2,n_2})^2\,(\bar{w}^{m_3,n_3})^2}{(-E^{m_1,n_1})\,\bar{w}^{m_1,n_1}}, \tag{183}$$

$$\delta w^{m_2,n_2} = \frac{3}{2}\,(\bar{m} - 1 - \bar{n}\,q_0)\,\mathcal{A}^{m_1,n_1}\,\mathcal{A}^{m_2,n_2}\,\mathcal{A}^{m_3,n_3} \times \frac{(\bar{w}^{m_1,n_1})^2\,(\bar{w}^{m_3,n_3})^2}{(-E^{m_2,n_2})\,\bar{w}^{m_2,n_2}}, \tag{184}$$

$$\delta w^{m_3,n_3} = \frac{3}{2}\,(\bar{m} - 1 - \bar{n}\,q_0)\,\mathcal{A}^{m_1,n_1}\,\mathcal{A}^{m_2,n_2}\,\mathcal{A}^{m_3,n_3} \times \frac{(\bar{w}^{m_1,n_1})^2\,(\bar{w}^{m_2,n_2})^2}{(-E^{m_3,n_3})\,\bar{w}^{m_3,n_3}}, \tag{185}$$

where use has been made of Eqs. (101)–(103).

Note that the modes phase lock in the most mutually destabilizing possible phase relation.[30] Thus, whereas, in the non-phase-locked state, the nonlinear interaction of the three coupled modes gives rise to a relatively small amplitude (because $\omega_0\,\tau_R \gg 1$) oscillation in the island widths, as described in Sec. IV G, the same interaction in the phase-locked state produces a time-independent increase in the three island widths that is $\mathcal{O}(\omega_0\,\tau_R\,\bar{w}) \gg 1$ larger that the amplitude of the aforementioned oscillation.

Incidentally, in the theory presented in this paper, it is impossible for phase locking to occur without the slip frequency being reduced to zero. The ultimate reason for this is the no-slip constraint introduced in Sec. II E. According to this constraint, each magnetic island is convected by the plasma at its rational surface. The no-slip constraint holds whenever the island width significantly exceeds the linear layer width.[37] In the opposite limit, the island can slip through the plasma at its rational surface, which would permit phase locking to occur without the slip frequency being reduced to zero. There is evidence from both experiment and numerical modeling that, under these circumstances, phase locking can give rise to a mutual, steady-state, stabilizing effect.[38] In this paper, it is assumed that the island widths of all coupled modes remain sufficiently large that the no-slip constraint is always applicable.

Let θ, ϕ be simultaneous solutions of

$$m_1\,\theta - n_1\,\phi + \varphi^{m_1,n_1} = 0, \tag{186}$$

$$m_2\,\theta - n_2\,\phi + \varphi^{m_2,n_2} = 0. \tag{187}$$

It follows from Sec. II E that one of the X-points of the m_1, n_1 island chain coincides with one of the X-points of the m_2, n_2 island chain at the angular position characterized by the poloidal and toroidal angles θ and ϕ, respectively. However, making use of Eqs. (81), (161), and (176), we can add the previous two equations to give

$$m_3\,\theta - n_3\,\phi + \varphi^{m_3,n_3} = 0. \tag{188}$$

This implies that one of the X-points of the m_3, n_3 island chain lies at the angular position θ, ϕ. In other words, the phase-locked state is such that one of the X-points of all three coupled island chains coincides permanently at the angular position specified by the simultaneous solution of Eqs. (186) and (187). It is easily demonstrated that this position rotates poloidally and toroidally at the angular velocities

$$\frac{d\theta}{dt} = \frac{-n_1\,n_2\left(\Omega_\phi^{m_2,n_2} - \Omega_\phi^{m_1,n_1}\right) + n_1\,m_2\,\Omega_\theta^{m_2,n_2} - m_1\,n_2\,\Omega_\theta^{m_1,n_1}}{n_1\,m_2 - m_1\,n_2}, \tag{189}$$

$$\frac{d\phi}{dt} = \frac{m_1\,m_2\left(\Omega_\theta^{m_2,n_2} - \Omega_\theta^{m_1,n_1}\right) + n_1\,m_2\,\Omega_\phi^{m_1,n_1} - m_1\,n_2\,\Omega_\phi^{m_2,n_2}}{n_1\,m_2 - m_1\,n_2}, \tag{190}$$

respectively. Likewise, it can be shown that the one of the O-points of all three island chains coincides permanently at the angular position specified by the simultaneous solution of

$$m_1\,\theta - n_1\,\phi + \varphi^{m_1,n_1} = \pi, \tag{191}$$

$$m_2\,\theta - n_2\,\phi + \varphi^{m_2,n_2} = \pi, \tag{192}$$

and that this position rotates poloidally and toroidally at the angular velocities (189) and (190), respectively. Note that, at the special angular positions at which the island chain X- and O-points coincide, the radial plasma displacements associated with the three tearing modes add in phase at the edge of the plasma. This behavior is reminiscent of the so-called "slinky mode" generated by the nonlinear phase locking of tearing modes in reversed-field pinches.[39–42]

V. TOROIDAL COUPLING OF TWO NEOCLASSICAL TEARING MODES

A. Introduction

Consider the coupling of two modes, resonant at two different rational surfaces within the plasma, via the 0, 1 perturbation associated with the Shafranov shift of the equilibrium magnetic flux-surfaces. Let the associated mode numbers be m, n and $m+1, n$, where $n > 0$. This type of coupling is generally known as *toroidal coupling* (because it couples tearing modes with a common toroidal mode number).[27–29] It follows from Eq. (63) that $\hat{r}^{m,n} < \hat{r}^{m+1,n}$. As before, it is assumed that $E^{m,n}, E^{m+1,n} < 0$, and $m > 1$, so that both resonant modes are conventional neoclassical tearing modes.

B. Nonlinear coupling

According to the analysis of Secs. II G and IV B, we can write

$$\mathcal{C}^{n,0,n}_{m,1,m+1} = \frac{3\,q_a}{2}\,(\bar{m} - 1 - \bar{n}\,q_0)\,\mathcal{A}^{m,n}\,\mathcal{A}^{1,0}\,\mathcal{A}^{m+1,n}, \tag{193}$$

where $\mathcal{A}^{1,0}$ takes the special value

$$\mathcal{A}^{1,0} = \left(\frac{q_a}{q_0}\right)^{1/2}, \tag{194}$$

and

$$\bar{m} = \frac{2\,(m+1)}{3}, \tag{195}$$

$$\bar{n} = \frac{2n}{3}. \tag{196}$$

Here, use has been made of Eqs. (17), (54), and (61). Note that $\bar{m} - 1 - \bar{n}\,q_0 > 0$ provided that

$$q_0 < \frac{m - 1/2}{n}, \tag{197}$$

as is assumed to be the case.

C. Island width evolution equations

Similarly to the analysis of Sec. IV C, the Rutherford island width evolution equations of the two coupled tearing modes take the form

$$\tau_R\,(\hat{r}^{\,m,n})^2\,\frac{dw^{m,n}}{dt} = E^{m,n} + \hat{\beta}_0\left(\frac{m}{n}\right)^2\frac{\sqrt{\hat{r}^{\,m,n}}}{w^{m,n}} + \frac{3}{2}\,(\bar{m} - 1 - \bar{n}\,q_0)\,\mathcal{A}^{m,n}\,\mathcal{A}^{1,0} \times \mathcal{A}^{m+1,n}\,\frac{\Delta_a^{1,0}\,(w^{m+1,n})^2}{(w^{m,n})^2}\,\cos\varphi, \tag{198}$$

$$\tau_R\,(\hat{r}^{\,m+1,n})^2\,\frac{dw^{m+1,n}}{dt} = E^{m+1,n} + \hat{\beta}_0\left(\frac{m+1}{n}\right)^2\frac{\sqrt{\hat{r}^{\,m+1,n}}}{w^{m+1,n}} + \frac{3}{2}\,(\bar{m} - 1 - \bar{n}\,q_0)\,\mathcal{A}^{m,n}\,\mathcal{A}^{1,0} \times \mathcal{A}^{m+1,n}\,\frac{(w^{m,n})^2\,\Delta_a^{1,0}}{(w^{m+1,n})^2}\,\cos\varphi, \tag{199}$$

where

$$\varphi = \varphi^{\,m,n} - \varphi^{\,m+1,n}. \tag{200}$$

D. Electromagnetic torques

Similarly to the analysis of Secs. II F and IV D, the normalized electromagnetic torques that develop at the two coupled rational surfaces are

$$\delta\hat{T}_{\rm EM}^{\,m,n} = -n\,\delta\hat{T}_{\rm EM}, \tag{201}$$

$$\delta\hat{T}_{\rm EM}^{\,m+1,n} = n\,\delta\hat{T}_{\rm EM}, \tag{202}$$

where

$$\delta\hat{T}_{\rm EM} = \frac{3}{2\,q_a^2}\,(\bar{m} - 1 - \bar{n}\,q_0)\,\mathcal{A}^{m,n}\,\mathcal{A}^{1,0}\,\mathcal{A}^{m+1,n} \times (w^{m,n})^2\,\Delta_a^{1,0}\,(w^{m+1,n})^2\,\sin\varphi. \tag{203}$$

E. Modified toroidal angular velocity profile

Similarly to the analysis of Sec. IV E, the modified toroidal angular velocity profile satisfies Eqs. (88) and (89), where

$$\left[\hat{r}\,\frac{\partial\Delta\Omega_\phi}{\partial\hat{r}}\right]_{\hat{r}_-^{\,m,n}}^{\hat{r}_+^{\,m,n}} = n\,T, \tag{204}$$

$$\left[\hat{r}\,\frac{\partial\Delta\Omega_\phi}{\partial\hat{r}}\right]_{\hat{r}_-^{\,m+1,n}}^{\hat{r}_+^{\,m+1,n}} = -n\,T, \tag{205}$$

and

$$T = \frac{3}{4}\,\frac{\epsilon^2\,\tau_M}{q_a^2\,\tau_H^2}\,(\bar{m} - 1 - \bar{n}\,q_0)\,\mathcal{A}^{m,n}\,\mathcal{A}^{1,0}\,\mathcal{A}^{m+1,n} \times (w^{m,n})^2\,\Delta_a^{1,0}\,(w^{m+1,n})^2\,\sin\varphi. \tag{206}$$

F. Slip frequency

Similarly to the analysis of Sec. IV F, we can write $d\varphi/dt = \omega$, where

$$\omega = -m\,\Omega_\theta^{m,n} + (m+1)\,\Omega_\theta^{m+1,n} + n\,\Omega_\phi^{m,n} - n\,\Omega_\phi^{m+1,n}, \tag{207}$$

and

$$\omega(t) = \omega_0 + n\,\Delta\Omega_\phi^{m,n}(t) - n\,\Delta\Omega_\phi^{m+1,n}(t). \tag{208}$$

G. Non-phase-locked state

In the non-phase-locked state, similarly to the analysis of Sec. IV G, we can write

$$w^{m,n}(t) \simeq \bar{w}^{\,m,n} + \delta w^{m,n}\,\sin\varphi(t), \tag{209}$$

$$w^{m+1,n}(t) \simeq \bar{w}^{\,m+1,n} + \delta w^{m+1,n}\,\sin\varphi(t), \tag{210}$$

where $\delta w^{m,n}/\bar{w}^{\,m,n} \ll 1$, etc. Here, $\bar{w}^{\,m,n}$ and $\bar{w}^{\,m+1,n}$ are specified by Eq. (101), and

$$\delta w^{m,n} = \frac{3}{2}\,\frac{1}{\omega\,\tau_R}\,(\bar{m} - 1 - \bar{n}\,q_0)\,\mathcal{A}^{m,n}\,\mathcal{A}^{1,0}\,\mathcal{A}^{m+1,n} \times \frac{\Delta_a^{1,0}\,(\bar{w}^{\,m+1,n})^2}{(\hat{r}^{\,m,n})^2\,(\bar{w}^{\,m,n})^2}, \tag{211}$$

$$\delta w^{m+1,n} = \frac{3}{2}\,\frac{1}{\omega\,\tau_R}\,(\bar{m} - 1 - \bar{n}\,q_0)\,\mathcal{A}^{m,n}\,\mathcal{A}^{1,0}\,\mathcal{A}^{m+1,n} \times \frac{(\bar{w}^{\,m,n})^2\,\Delta_a^{1,0}}{(\hat{r}^{\,m+1,n})^2\,(\bar{w}^{\,m+1,n})^2}. \tag{212}$$

The constraints $\delta w^{m,n}/\bar{w}^{\,m,n} \ll 1$, etc., imply that

$$\omega\,\tau_R \gg \frac{3}{2}\,(\bar{m} - 1 - \bar{n}\,q_0)\,\mathcal{A}^{m,n}\,\mathcal{A}^{1,0}\,\mathcal{A}^{m+1,n} \times \frac{\Delta_a^{1,0}\,(\bar{w}^{\,m+1,n})^2}{(\hat{r}^{\,m,n})^2\,(\bar{w}^{\,m,n})^3}, \tag{213}$$

etc.

The time-averaged component of the electromagnetic torque can be written $\langle T\rangle = \delta T$, where

$$\delta T = \frac{3^2}{2^3}\frac{\epsilon^2}{q_a^2}\frac{\tau_M}{\omega\,\tau_R\,\tau_H^2}\,(\bar m - 1 - \bar n\,q_0)^2\,(\mathcal{A}^{m,n}\,\mathcal{A}^{1,0}\,\mathcal{A}^{m+1,n})^2 \times\left[\frac{(\Delta_a^{1,0})^2\,(\bar w^{\,m+1,n})^4}{(\hat r^{\,m,n})^2\,\bar w^{\,m,n}}+\frac{(\bar w^{\,m,n})^4\,(\Delta_a^{1,0})^2}{(\hat r^{\,m+1,n})^2\,\bar w^{\,m+1,n}}\right]. \tag{214}$$

As before, assuming that the plasma toroidal rotation profile only responds appreciably to the time-averaged torque, we can write $\Delta\Omega_\phi(\hat r,t)=\Delta\Omega_\phi(\hat r)$, where $\Delta\Omega_\phi(\hat r)$ satisfies Eqs. (116) and (117), as well as

$$\left[\hat r\,\frac{d\Delta\Omega_\phi}{d\hat r}\right]_{\hat r_-^{\,m,n}}^{\hat r_+^{\,m,n}} = n\,\delta T, \tag{215}$$

$$\left[\hat r\,\frac{d\Delta\Omega_\phi}{d\hat r}\right]_{\hat r_-^{\,m+1,n}}^{\hat r_+^{\,m+1,n}} = -n\,\delta T. \tag{216}$$

The solution to these equations is

$$\Delta\Omega_\phi(\hat r) = \Delta\Omega_\phi^{m,n}, \tag{217}$$

for $0\le\hat r\le\hat r^{\,m,n}$, and

$$\Delta\Omega_\phi(\hat r) = \Delta\Omega_\phi^{m,n}\,\frac{\ln\left(\hat r/\hat r^{\,m+1,n}\right)}{\ln\left(\hat r^{\,m,n}/\hat r^{\,m+1,n}\right)}, \tag{218}$$

for $\hat r^{\,m,n}<\hat r\le\hat r^{\,m+1,n}$, and

$$\Delta\Omega_\phi(\hat r) = 0, \tag{219}$$

for $\hat r>\hat r^{\,m+1,n}$, where

$$\Delta\Omega_\phi^{m,n} = -n\ln\left(\frac{\hat r^{\,m+1,n}}{\hat r^{\,m,n}}\right)\delta T, \tag{220}$$

$$\Delta\Omega_\phi^{m+1,n} = 0, \tag{221}$$

which implies that

$$\omega = \omega_0 - n^2\ln\left(\frac{\hat r^{\,m+1,n}}{\hat r^{\,m,n}}\right)\delta T. \tag{222}$$

Note that the modification to the plasma toroidal angular velocity profile is localized to the region of the plasma lying within the outermost coupled rational surface.

Combining Eqs. (214) and (222), we obtain the torque balance equation

$$4\,(1-\hat\omega)\,\hat\omega = F, \tag{223}$$

where $\hat\omega=\omega/\omega_0$, and

$$F = \frac{3^2}{2}\frac{\epsilon^2}{q_a^2}\frac{\tau_M}{\tau_R\,(\omega_0\,\tau_H)^2}\left[n^2\ln\left(\frac{\hat r^{\,m+1,n}}{\hat r^{\,m,n}}\right)\right](\bar m - 1 - \bar n\,q_0)^2 \times(\mathcal{A}^{m,n}\,\mathcal{A}^{1,0}\,\mathcal{A}^{m+1,n})^2\,\mathcal{W}, \tag{224}$$

with

$$\mathcal{W} = \frac{(\Delta_a^{1,0})^2\,(\bar w^{\,m+1,n})^4}{(\hat r^{\,m,n})^2\,\bar w^{\,m,n}}+\frac{(\bar w^{\,m,n})^4\,(\Delta_a^{1,0})^2}{(\hat r^{\,m+1,n})^2\,\bar w^{\,m+1,n}}. \tag{225}$$

As described in Sec. IV G, when F reaches the critical value unity, at which point the slip frequency has been reduced to one half of its unperturbed value, there is a bifurcation to a phase-locked state.

H. Phase-locked state

Following the analysis of Sec. IV I, the phase-locked state is characterized by $\omega=0$, and

$$\varphi(t) = \varphi_0, \tag{226}$$

where φ_0 is a constant. Thus, Eqs. (207) and (208) yield

$$0 = -m\,\Omega_\theta^{m,n} + (m+1)\,\Omega_\theta^{m+1,n} + n\,\Omega_\phi^{m,n} - n\,\Omega_\phi^{m+1,n}, \tag{227}$$

$$0 = \omega_0 + n\,\Delta\Omega_\phi^{m,n} - n\,\Delta\Omega_\phi^{m+1,n}, \tag{228}$$

respectively. If the plasma rotates poloidally as a solid body [i.e., $\Omega_\theta(\hat r)=\Omega_\theta$], as is likely to be the case in the plasma core, then Eq. (227) implies that

$$\Omega_\phi^{m,n} = \Omega_\phi^{m+1,n} - \frac{\Omega_\theta}{n}. \tag{229}$$

In other words, the phase-locked state is characterized by a toroidal velocity profile in the plasma core that is either flattened (if Ω_θ is negligible) or inverted (assuming that Ω_θ and Ω_ϕ have the same sign). This entails a substantial loss of core momentum confinement.

In the phase-locked state, we expect $\Delta\Omega_\phi(\hat r,t)=\Delta\Omega_\phi(\hat r)$. Thus, the modified plasma toroidal angular velocity profile is governed by Eqs. (116) and (117), where

$$\left[\hat r\,\frac{d\Delta\Omega_\phi}{d\hat r}\right]_{\hat r_-^{\,m,n}}^{\hat r_+^{\,m,n}} = n\,T_0, \tag{230}$$

$$\left[\hat r\,\frac{d\Delta\Omega_\phi}{d\hat r}\right]_{\hat r_-^{\,m+1,n}}^{\hat r_+^{\,m+1,n}} = -n\,T_0, \tag{231}$$

and

$$T_0 = \frac{3}{4}\frac{\epsilon^2\,\tau_M}{q_a^2\,\tau_H^2}\,(\bar m - 1 - \bar n\,q_0)\,\mathcal{A}^{m,n}\,\mathcal{A}^{1,0}\,\mathcal{A}^{m+1,n} \times(\bar w^{\,m,n})^2\,\Delta_a^{1,0}\,(\bar w^{\,m+1,n})^2\,\sin\varphi_0. \tag{232}$$

The solution of Eqs. (116), (117), (230), and (231) is given by Eqs. (217)–(219), where

$$\Delta\Omega_\phi^{m,n} = -n\ln\left(\frac{\hat r^{\,m+1,n}}{\hat r^{\,m,n}}\right)T_0, \tag{233}$$

$$\Delta\Omega_\phi^{m+1,n} = 0. \tag{234}$$

Thus, it follows from Eqs. (224), (228), and (232) that

$$\frac{\Delta\Omega_\phi^{m,n}}{\omega_0} = -\frac{1}{n}, \tag{235}$$

$$\frac{\Delta\Omega_\phi^{m+1,n}}{\omega_0}=0, \tag{236}$$

and

$$\sin\varphi_0=\frac{4\,G}{F}, \tag{237}$$

where

$$G=\frac{3}{2}\,\frac{1}{\omega_0\,\tau_R}\,(\bar m-1-\bar n\,q_0)\,\mathcal{A}^{m,n}\,\mathcal{A}^{1,0}\,\mathcal{A}^{m+1,n}\times\left[\frac{\Delta_a^{1,0}\,(\bar w^{\,m+1,n})^2}{(\hat r^{\,m,n})^2\,(\bar w^{\,m,n})^3}+\frac{(\bar w^{\,m,n})^2\,\Delta_a^{1,0}}{(\hat r^{\,m+1,n})^2\,(\bar w^{\,m+1,n})^3}\right]. \tag{238}$$

Now, we know that $F\geq 1$ in the phase-locked state. Moreover, Eq. (213) implies that $G\ll 1$. Hence, Eq. (237) yields

$$\sin\varphi_0\simeq 0. \tag{239}$$

As before, the dynamically stable solution of this equation is

$$\varphi_0\simeq 0. \tag{240}$$

According to Eqs. (198), (199), (226), and (240), the Rutherford island width evolution equations of the two coupled tearing modes in the phase-locked state take the form

$$\tau_R\,(\hat r^{\,m,n})^2\,\frac{dw^{m,n}}{dt}\simeq E^{m,n}+\hat\beta_0\left(\frac{m}{n}\right)^2\frac{\sqrt{\hat r^{\,m,n}}}{w^{m,n}}+\frac{3}{2}\,(\bar m-1-\bar n\,q_0)\,\mathcal{A}^{m,n}\,\mathcal{A}^{1,0}\times\mathcal{A}^{m+1,n}\,\frac{\Delta_a^{1,0}\,(w^{m+1,n})^2}{(w^{m,n})^2}, \tag{241}$$

$$\tau_R\,(\hat r^{\,m+1,n})^2\,\frac{dw^{m+1,n}}{dt}\simeq E^{m+1,n}+\hat\beta_0\left(\frac{m+1}{n}\right)^2\frac{\sqrt{\hat r^{\,m+1,n}}}{w^{m+1,n}}+\frac{3}{2}\,(\bar m-1-\bar n\,q_0)\,\mathcal{A}^{m,n}\,\mathcal{A}^{1,0}\times\mathcal{A}^{m+1,n}\,\frac{(w^{m,n})^2\,\Delta_a^{1,0}}{(w^{m+1,n})^2}. \tag{242}$$

Thus, writing

$$w^{m,n}(t)\simeq\bar w^{\,m,n}+\delta w^{m,n}, \tag{243}$$

$$w^{m+1,n}(t)\simeq\bar w^{\,m+1,n}+\delta w^{m+1,n}, \tag{244}$$

we obtain

$$\delta w^{m,n}=\frac{3}{2}\,(\bar m-1-\bar n\,q_0)\,\mathcal{A}^{m,n}\,\mathcal{A}^{1,0}\,\mathcal{A}^{m+1,n}\,\frac{\Delta_a^{1,0}\,(\bar w^{\,m+1,n})^2}{(-E^{m,n})\,\bar w^{\,m,n}}, \tag{245}$$

$$\delta w^{m+1,n}=\frac{3}{2}\,(\bar m-1-\bar n\,q_0)\,\mathcal{A}^{m,n}\,\mathcal{A}^{1,0}\,\mathcal{A}^{m+1,n}\times\frac{(\bar w^{\,m,n})^2\,\Delta_a^{1,0}}{(-E^{m+1,n})\,\bar w^{\,m+1,n}}, \tag{246}$$

where use has been made of Eq. (101).

As previously, the two tearing modes phase lock in the most mutually destabilizing possible phase relation. Furthermore, whereas, in the non-phase-locked state, the nonlinear interaction of the two coupled modes gives rise to a relatively small amplitude oscillation in the island widths, the same interaction in the phase-locked state produces a time-independent increase in the two island widths that is much larger that the amplitude of the aforementioned oscillation.

Let θ,ϕ be simultaneous solutions of

$$m\,\theta-n\,\phi+\varphi^{m,n}=0, \tag{247}$$

$$(m+1)\,\theta-n\,\phi+\varphi^{m+1,n}=0. \tag{248}$$

It follows that one of the X-points of the m, n island chain coincides with one of the X-points of the $m+1,n$ island chain at the angular position characterized by the poloidal and toroidal angles θ and ϕ, respectively. However, making use of Eqs. (200), (226), and (240), we can solve the previous two equations to give

$$\theta=0, \tag{249}$$

$$\phi=\frac{\varphi^{m+1,n}}{n}. \tag{250}$$

In other words, in the phase-locked state, one of the X-points of the two coupled island chains coincides permanently on the outboard mid-plane (i.e., $\theta=0$). Moreover, the two X-points rotate toroidally at the angular velocity

$$\frac{d\phi}{dt}=-\left(\frac{m+1}{n}\right)\Omega_\theta^{m+1,n}+\Omega_\phi^{m+1,n}. \tag{251}$$

Likewise, it can be shown that one of the O-points of the two coupled island chains also coincides permanently on the outboard mid-plane at the toroidal angle

$$\phi=\frac{\varphi^{m+1,n}-\pi}{n}, \tag{252}$$

and that the two O-points rotate toroidally at the angular velocity (251). The prediction that toroidally coupled tearing modes phase lock in a configuration in which their X- and O-points coincide permanently on the outboard mid-plane is in accordance with experimental observations.[43]

VI. NONLINEAR TOROIDAL COUPLING OF TWO NEOCLASSICAL TEARING MODES

A. Introduction

It is possible for two tearing modes possessing different toroidal mode numbers to phase lock via a combination of non-linear and toroidal coupling. Let $2m-1,2n$ and m, n be the associated mode numbers, where $m>1$ and $n>0$. The coupling proceeds in two stages. First, the m, n mode couples nonlinearly to itself to produce a $2m,2n$ mode. Second, the $2m,2n$ mode couples toroidally to the $2m-1,2n$ mode. It follows from Eq. (63) that $\hat r^{\,2m-1,2n}<\hat r^{\,m,n}$. As before, it is

assumed that $E^{2m-1,2n}, E^{m,n} < 0$, and $m > 1$, so that both coupled modes are neoclassical tearing modes. It is also assumed that $E^{2m,2n} < 0$ (because this is inevitably the case if $E^{m,n} < 0$).

B. Nonlinear coupling

According to the analysis of Sec. II G, we can write

$$\Delta\Psi^{2m-1,2n} = E^{2m-1,2n}\,\Psi^{2m-1,2n} + \mathcal{C}^{2n,0,2n}_{2m-1,1,2m}\,(\Psi^{1,0})^*\,\Psi^{2m,2n}, \tag{253}$$

$$\Delta\Psi^{m,n} = E^{m,n}\,\Psi^{m,n} + \mathcal{C}^{n,n,2n}_{m,m,2m}\,(\Psi^{m,n})^*\,\Psi^{2m,2n}, \tag{254}$$

$$\Delta\Psi^{2m,2n} = E^{2m,2n}\,\Psi^{2m,2n} + \mathcal{C}^{2n,0,2n}_{2m-1,1,2m}\,\Psi^{2m-1,2n}\,\Psi^{1,0} + \mathcal{C}^{n,n,2n}_{m,m,2m}\,(\Psi^{m,n})^2, \tag{255}$$

where $\Psi^{1,0} = \Delta_a^{1,0}/q_a$. Setting $\Delta\Psi^{2m,2n} = 0$, which ensures that there is no $2m, 2n$ current sheet at the m, n rational surface, we obtain

$$\Psi^{2m,2n} = \frac{\mathcal{C}^{2n,0,2n}_{2m-1,1,2m}}{(-E^{2m,2n})}\,\Psi^{2m-1,2n}\,\Psi^{1,0} + \frac{\mathcal{C}^{n,n,2n}_{m,m,2m}}{(-E^{2m,2n})}\,(\Psi^{m,n})^2, \tag{256}$$

as our expression for the equilibrium $2m, 2n$ magnetic flux driven at the rational surface due to nonlinear coupling with the $2m-1, 2n$ and m, n modes. Note that $|\Psi^{2m,2n}|/|\Psi^{m,n}| \ll 1$, assuming that $|\Psi^{m,n}|, |\Psi^{2m-1,2n}|, |\Psi^{1,0}| \ll 1$ (i.e., the $2m-1, 2n$ and m, n island widths, as well as the edge Shafranov shift, are all relatively small compared to the plasma minor radius), which ensures that the magnetic island at the m, n rational surface predominately has the helicity m, n, rather than $2m, 2n$. Equations (253), (254), and (256) yield

$$\Delta\Psi^{2m-1,2n} = \tilde{E}^{2m-1,2n}\,\Psi^{2m-1,2n} + \frac{\mathcal{C}^{n,n,2n}_{m,m,2m}\,\mathcal{C}^{2n,0,2n}_{2m-1,1,2m}}{(-E^{2m,2n})}\,(\Psi^{1,0})^*\,(\Psi^{m,n})^2, \tag{257}$$

$$\Delta\Psi^{m,n} = \tilde{E}^{m,n}\,\Psi^{m,n} + \frac{\mathcal{C}^{n,n,2n}_{m,m,2m}\,\mathcal{C}^{2n,0,2n}_{2m-1,1,2m}}{(-E^{2m,2n})} \times (\Psi^{m,n})^*\,\Psi^{1,0}\,\Psi^{2m-1,2n}, \tag{258}$$

where

$$\tilde{E}^{2m-1,2n} = E^{2m-1,2n} + \frac{\left(\mathcal{C}^{2n,0,2n}_{2m-1,1,2m}\,\Delta_a^{1,0}/q_a\right)^2}{(-E^{2m,2n})}, \tag{259}$$

$$\tilde{E}^{m,n} = E^{m,n} + \frac{\left[\mathcal{C}^{n,n,2n}_{m,m,2m}\,(w^{m,n})^2/q_a\right]^2}{(-E^{2m,2n})}. \tag{260}$$

However

$$\mathcal{C}^{n,n,2n}_{m,m,2m} = \frac{3\,q_a}{2}\,(\bar{m} - 1 - \bar{n}\,q_0)\,\mathcal{A}^{m,n}\,\mathcal{A}^{m,n}\,\mathcal{A}^{2m,2n}, \tag{261}$$

$$\mathcal{C}^{2n,0,2n}_{2m-1,1,2m} = \frac{3\,q_a}{2}\,(\bar{m} - 1 - \bar{n}\,q_0)\,\mathcal{A}^{2m-1,2n}\,\mathcal{A}^{1,0}\,\mathcal{A}^{2m,2n}, \tag{262}$$

where

$$\bar{m} = \frac{4\,m}{3}, \tag{263}$$

$$\bar{n} = \frac{4\,n}{3}. \tag{264}$$

Note that $\bar{m} - 1 - \bar{n}\,q_0 > 0$ provided that

$$q_0 < \frac{m - 3/4}{n}, \tag{265}$$

as is assumed to be the case.

C. Island width evolution equations

Similarly to the analysis of Sec. IV C, the Rutherford island width evolutions equations of the two coupled tearing modes take the form

$$\tau_R\,(\hat{r}^{2m-1,2n})^2\,\frac{dw^{2m-1,2n}}{dt} = \tilde{E}^{2m-1,2n} + \hat{\beta}_0\left(\frac{2m-1}{2n}\right)^2 \times \frac{\sqrt{\hat{r}^{2m-1,2n}}}{w^{2m-1,2n}} + \mathcal{B}\,\frac{(w^{m,n})^4}{(w^{2m-1,2n})^2}\,\cos\varphi, \tag{266}$$

$$\tau_R\,(\hat{r}^{m,n})^2\,\frac{dw^{m,n}}{dt} = \tilde{E}^{m,n} + \hat{\beta}_0\left(\frac{m}{n}\right)^2\,\frac{\sqrt{\hat{r}^{m,n}}}{w^{m,n}} + \mathcal{B}\,(w^{2m-1,2n})^2\,\cos\varphi, \tag{267}$$

where

$$\mathcal{B} = \frac{3^2}{2^2}\,(\bar{m} - 1 - \bar{n}\,q_0)^2\,(\mathcal{A}^{m,n})^2\,(\mathcal{A}^{2m,2n})^2 \times \mathcal{A}^{1,0}\,\mathcal{A}^{2m-1,2n}\,\frac{\Delta_a^{1,0}}{(-E^{2m,2n})}, \tag{268}$$

and

$$\varphi = \varphi^{2m-1,2n} - 2\,\varphi^{m,n}. \tag{269}$$

D. Electromagnetic torques

Similarly to the analysis of Secs. II F and IV D, the normalized electromagnetic torques that develop at the two rational surfaces are

$$\delta\hat{T}^{2m-1,2n}_{\rm EM} = -2n\,\delta\hat{T}_{\rm EM}, \tag{270}$$

$$\delta\hat{T}^{m,n}_{\rm EM} = 2n\,\delta\hat{T}_{\rm EM}, \tag{271}$$

where

$$\delta\hat{T}_{\rm EM} = \frac{\mathcal{B}}{q_a^2}\,(w^{2m-1,2n})^2\,(w^{m,n})^4\,\sin\varphi. \tag{272}$$

E. Modified toroidal angular velocity profile

Similarly to the analysis of Sec. IV E, the modified toroidal angular velocity profile satisfies Eqs. (88) and (89), where

$$\left[\hat{r}\,\frac{\partial \Delta\Omega_\phi}{\partial \hat{r}}\right]_{\hat{r}_-^{2m-1,2n}}^{\hat{r}_+^{2m-1,2n}} = n\,T, \tag{273}$$

$$\left[\hat{r}\,\frac{\partial \Delta\Omega_\phi}{\partial \hat{r}}\right]_{\hat{r}_-^{m,n}}^{\hat{r}_+^{m,n}} = -n\,T, \tag{274}$$

and

$$T = \frac{\epsilon^2\,\tau_M}{q_a^2\,\tau_H^2}\,\mathcal{B}\,(w^{2m-1,2n})^2\,(w^{m,n})^4\,\sin\varphi. \tag{275}$$

F. Slip frequency

Similarly to the analysis of Sec. IV F, we can write $d\varphi/dt = \omega$, where

$$\omega = -(2m-1)\,\Omega_\theta^{2m-1,2n} + 2m\,\Omega_\theta^{m,n} + 2n(\Omega_\phi^{2m-1,2n} - \Omega_\phi^{m,n}), \tag{276}$$

and

$$\omega(t) = \omega_0 + 2n(\Delta\Omega_\phi^{2m-1,2n} - \Delta\Omega_\phi^{m,n}). \tag{277}$$

G. Non-phase-locked state

In the non-phase-locked state, similarly to the analysis of Sec. IV G, we can write

$$w^{2m-1,2n}(t) \simeq \bar{w}^{2m-1,2n} + \delta w^{2m-1,2n}\,\sin\varphi(t), \tag{278}$$

$$w^{m,n}(t) \simeq \bar{w}^{m,n} + \delta w^{m,n}\,\sin\varphi(t), \tag{279}$$

where $\delta w^{2m-1,2n}/\bar{w}^{2m-1,2n} \ll 1$, etc.. Here, $\bar{w}^{2m-1,2n}$ and $\bar{w}^{m,n}$ are specified by Eq. (101) (except that $E^{2m-1,2n}$ is replaced by $\tilde{E}^{2m-1,2n}$, etc.), and

$$\delta w^{2m-1,2n} = \frac{\mathcal{B}}{\omega\,\tau_R}\,\frac{(\bar{w}^{m,n})^4}{(\hat{r}^{2m-1,2n})^2\,(\bar{w}^{2m-1,2n})^2}, \tag{280}$$

$$\delta w^{m,n} = \frac{\mathcal{B}}{\omega\,\tau_R}\,\frac{(\bar{w}^{2m-1,2n})^2}{(\hat{r}^{m,n})^2}. \tag{281}$$

The constraints $\delta w^{2m-1,2n}/\bar{w}^{2m-1,2n} \ll 1$, etc., imply that

$$\omega\,\tau_R \gg \mathcal{B}\,\frac{(\bar{w}^{m,n})^4}{(\hat{r}^{2m-1,2n})^2\,(\bar{w}^{2m-1,2n})^3}, \mathcal{B}\,\frac{(\bar{w}^{2m-1,2n})^2}{(\hat{r}^{m,n})^2\,\bar{w}^{m,n}}. \tag{282}$$

The time-averaged component of the electromagnetic torque can be written $\langle T\rangle = \delta T$, where

$$\delta T = \frac{\epsilon^2}{q_a^2}\,\frac{\tau_M}{\omega\,\tau_R\,\tau_H^2}\,\mathcal{B}^2\left[\frac{(\bar{w}^{m,n})^8}{(\hat{r}^{2m-1,2n})^2\,\bar{w}^{2m-1,2n}} + \frac{2\,(\bar{w}^{2m-1,2n})^4\,(\bar{w}^{m,n})^3}{(\hat{r}^{m,n})^2}\right]. \tag{283}$$

As before, assuming that the plasma toroidal angular velocity profile only responds appreciably to the time-averaged torque, we can write $\Delta\Omega_\phi(\hat{r},t) = \Delta\Omega_\phi(\hat{r})$, where $\Delta\Omega_\phi(\hat{r})$ satisfies Eqs. (116) and (117), as well as

$$\left[\hat{r}\,\frac{d\Delta\Omega_\phi}{d\hat{r}}\right]_{\hat{r}_-^{2m-1,2n}}^{\hat{r}_+^{2m-1,2n}} = n\,\delta T, \tag{284}$$

$$\left[\hat{r}\,\frac{d\Delta\Omega_\phi}{d\hat{r}}\right]_{\hat{r}_-^{m,n}}^{\hat{r}_+^{m,n}} = -n\,\delta T. \tag{285}$$

The solution to these equations is

$$\Delta\Omega_\phi(\hat{r}) = \Delta\Omega_\phi^{2m-1,2n}, \tag{286}$$

for $0 \le \hat{r} \le \hat{r}^{2m-1,2n}$, and

$$\Delta\Omega_\phi(\hat{r}) = \Delta\Omega_\phi^{2m-1,2n}\,\frac{\ln(\hat{r}/\hat{r}^{m,n})}{\ln(\hat{r}^{2m-1,2n}/\hat{r}^{m,n})}, \tag{287}$$

for $\hat{r}^{2m-1,2n} < \hat{r} \le \hat{r}^{m,n}$, and

$$\Delta\Omega_\phi(\hat{r}) = 0, \tag{288}$$

for $\hat{r} > \hat{r}^{m,n}$, where

$$\Delta\Omega_\phi^{2m-1,2n} = -n\ln\left(\frac{\hat{r}^{m,n}}{\hat{r}^{2m-1,2n}}\right)\delta T, \tag{289}$$

$$\Delta\Omega_\phi^{m,n} = 0, \tag{290}$$

which implies that

$$\omega = \omega_0 - 2n^2\ln\left(\frac{\hat{r}^{m,n}}{\hat{r}^{2m-1,2n}}\right)\delta T. \tag{291}$$

Note that the modification to the plasma toroidal angular velocity profile is localized to the region of the plasma lying within the outermost coupled rational surface.

Combining Eqs. (283) and (291), we obtain the torque balance equation

$$4\,(1-\hat{\omega})\,\hat{\omega} = F, \tag{292}$$

where $\hat{\omega} = \omega/\omega_0$, and

$$F = 2^3\,\frac{\epsilon^2}{q_a^2}\,\frac{\tau_M}{\tau_R\,(\omega_0\,\tau_H)^2}\left[n^2\ln\left(\frac{\hat{r}^{m,n}}{\hat{r}^{2m-1,2n}}\right)\right]\mathcal{B}^2\,\mathcal{W}, \tag{293}$$

with

$$\mathcal{W} = \frac{(\bar{w}^{m,n})^8}{(\hat{r}^{2m-1,2n})^2\,\bar{w}^{2m-1,2n}} + \frac{2\,(\bar{w}^{2m-1,2n})^4\,(\bar{w}^{m,n})^3}{(\hat{r}^{m,n})^2}. \tag{294}$$

As described in Sec. IV G, when F reaches the critical value unity, at which point the slip frequency has been reduced to one half of its unperturbed value, there is a bifurcation to a phase-locked state.

H. Phase-locked state

Following the analysis of Sec. IV I, the phase-locked state is characterized by $\omega = 0$, and

$$\varphi(t) = \varphi_0, \tag{295}$$

where φ_0 is a constant. Thus, Eqs. (276) and (277) yield

$$0 = -(2m-1)\,\Omega_\theta^{2m-1,2n} + 2m\,\Omega_\theta^{m,n} + 2n(\Omega_\phi^{2m-1,2n} - \Omega_\phi^{m,n}), \tag{296}$$

$$0 = \omega_0 + 2n(\Delta\Omega_\phi^{2m-1,2n} - \Delta\Omega_\phi^{m,n}), \tag{297}$$

respectively. If the plasma rotates poloidally as a solid body [i.e., $\Omega_\theta(\hat{r}) = \Omega_\theta$], as is likely to be the case in the plasma core, then Eq. (296) implies that

$$\Omega_\phi^{2m-1,2n} = \Omega_\phi^{m,n} - \frac{\Omega_\theta}{2n}. \tag{298}$$

In other words, the phase-locked state is characterized by a toroidal velocity profile in the plasma core that is either flattened or inverted. This entails a substantial loss of core momentum confinement.

In the phase-locked state, we expect $\Delta\Omega_\phi(\hat{r},t) = \Delta\Omega_\phi(\hat{r})$. Thus, the modified plasma toroidal angular velocity profile is governed by Eqs. (116) and (117), where

$$\left[\hat{r}\,\frac{d\Delta\Omega_\phi}{d\hat{r}}\right]_{\hat{r}_-^{2m-1,2n}}^{\hat{r}_+^{2m-1,2n}} = n\,T_0, \tag{299}$$

$$\left[\hat{r}\,\frac{d\Delta\Omega_\phi}{d\hat{r}}\right]_{\hat{r}_-^{m,n}}^{\hat{r}_+^{m,n}} = -n\,T_0, \tag{300}$$

and

$$T_0 = \frac{\epsilon^2\,\tau_M}{q_a^2\,\tau_H^2}\,\mathcal{B}\,(\bar{w}^{\,2m-1,2n})^2\,(\bar{w}^{\,m,n})^4\,\sin\varphi_0. \tag{301}$$

The solution of Eqs. (116), (117), (299), and (300) is given by Eqs. (286)–(288), where

$$\Delta\Omega_\phi^{2m-1,2n} = -n\ln\left(\frac{\hat{r}^{\,m,n}}{\hat{r}^{\,2m-1,2n}}\right)T_0, \tag{302}$$

$$\Delta\Omega_\phi^{m,n} = 0. \tag{303}$$

Thus, it follows from Eqs. (293), (297), and (301) that

$$\frac{\Delta\Omega_\phi^{2m-1,2n}}{\omega_0} = -\frac{1}{2n}, \tag{304}$$

$$\frac{\Delta\Omega_\phi^{m,n}}{\omega_0} = 0, \tag{305}$$

and

$$\sin\varphi_0 = \frac{4\,G}{F}, \tag{306}$$

where

$$G = \frac{\mathcal{B}}{\omega_0\,\tau_R}\left[\frac{(w^{m,n})^4}{(\hat{r}^{\,2m-1,2n})^2\,(\bar{w}^{\,2m-1,2n})^3} + \frac{2\,(\bar{w}^{\,2m-1,2n})^2}{(\hat{r}^{\,m,n})^2\,\bar{w}^{\,m,n}}\right]. \tag{307}$$

Now, we know that $F \geq 1$ in the phase-locked state. Moreover, Eq. (282) implies that $G \ll 1$. Hence, Eq. (306) yields

$$\sin\varphi_0 \simeq 0. \tag{308}$$

As before, the dynamically stable solution of this equation is

$$\varphi_0 \simeq 0. \tag{309}$$

According to Eqs. (266), (267), (295), and (309), the Rutherford island width evolution equations of the two coupled tearing modes in the phase-locked state take the form

$$\tau_R\,(\hat{r}^{\,2m-1,2n})^2\,\frac{dw^{\,2m-1,2n}}{dt} \simeq \tilde{E}^{\,2m-1,2n} + \hat{\beta}_0\left(\frac{2m-1}{2n}\right)^2 \times\frac{\sqrt{\hat{r}^{\,2m-1,2n}}}{w^{\,2m-1,2n}} + \mathcal{B}\,\frac{(w^{m,n})^4}{(w^{\,2m-1,2n})^2}, \tag{310}$$

$$\tau_R\,(\hat{r}^{\,m,n})^2\,\frac{dw^{\,m,n}}{dt} \simeq \tilde{E}^{\,m,n} + \hat{\beta}_0\left(\frac{m}{n}\right)^2\frac{\sqrt{\hat{r}^{\,m,n}}}{w^{\,m,n}} + \mathcal{B}\,(w^{\,2m-1,2n})^2. \tag{311}$$

Thus, writing

$$w^{\,2m-1,2n}(t) \simeq \bar{w}^{\,2m-1,2n} + \delta w^{\,2m-1,2n}, \tag{312}$$

$$w^{\,m,n}(t) \simeq \bar{w}^{\,2m-1,2n} + \delta w^{\,m,n}, \tag{313}$$

we obtain

$$\delta w^{\,2m-1,2n} = \mathcal{B}\,\frac{(\bar{w}^{\,m,n})^4}{(-\tilde{E}^{\,2m-1,2n})\,\bar{w}^{\,2m-1,2n}}, \tag{314}$$

$$\delta w^{\,m,n} = \mathcal{B}\,\frac{(\bar{w}^{\,2m-1,2n})^2\,\bar{w}^{\,m,n}}{(-\tilde{E}^{\,m,n})}, \tag{315}$$

where use has been made of Eq. (101) [with $E^{\,m,n}$ replaced by $\tilde{E}^{\,m,n}$, etc.].

As previously, the two tearing modes phase lock in the most mutually destabilizing possible phase relation. Furthermore, whereas, in the non-phase-locked state, the nonlinear interaction of the two coupled modes gives rise to a relatively small amplitude oscillation in the island widths, the same interaction in the phase-locked state produces a time-independent increase in the two island widths that is much larger that the amplitude of the aforementioned oscillation.

Let θ, ϕ be simultaneous solutions of

$$(2m-1)\,\theta - 2n\,\phi + \varphi^{\,2m-1,2n} = 0, \tag{316}$$

$$m\,\theta - n\,\phi + \varphi^{\,m,n} = 0. \tag{317}$$

It follows that one of the X-points of the $2m-1, 2n$ island chain coincides with one of the X-points of the m, n island chain at the angular position characterized by the poloidal and toroidal angles θ and ϕ, respectively. However, making use of Eqs. (269), (295), and (309), we can solve the previous two equations to give

$$\theta = 0, \tag{318}$$

$$\phi = \frac{\varphi^{\,m,n}}{n}. \tag{319}$$

In other words, in the phase-locked state, one of the X-points of the two coupled island chains coincides permanently on the outboard mid-plane (i.e., $\theta = 0$). Moreover, the two X-points rotate toroidally at the angular velocity

$$\frac{d\phi}{dt} = -\left(\frac{m}{n}\right)\Omega_\theta^{m,n} + \Omega_\phi^{m,n}. \tag{320}$$

Likewise, it can be shown that one of the O-points of the two coupled island chains also coincides permanently on the inboard mid-plane at the toroidal angle

$$\phi = \frac{\varphi^{m,n} + (m-1)\,\pi}{n}, \tag{321}$$

and that the two O-points rotate toroidally at the angular velocity (320).

I. Discussion

The type of nonlinear toroidal coupling described in this section has been observed in both the JET and the DIII-D tokamaks.[21,22] To be more exact, in both cases, the 3, 2 and 2, 1 neoclassical tearing modes are observed to phase lock to one another. This phase locking is inferred to take place in two stages. First, the 2, 1 mode couples to itself to produce a 4, 2 mode. Second, the 4, 2 mode couples toroidally to the 3, 2 mode. In accordance with the previous analysis, the observed phase-locked state is such that $\varphi^{3,2} = 2\,\varphi^{2,1}$, which necessitates a toroidal angular velocity profile in the plasma core that is either flattened or inverted (as is observed to be the case). In further accordance, the phase-locking bifurcation is observed to take place when the slip frequency has been reduced to about one half of its original value, the modification to the toroidal velocity profile is localized to the region interior to the 2, 1 rational surface, and the phase-locked state is such that one of the X-points of the 3, 2 and 2, 1 island chains coincides permanently on the outboard mid-plane.

VII. PHASE-LOCKING THRESHOLDS

A. Definitions

It is helpful to define the conventional plasma beta parameter

$$\beta = \frac{\langle p\rangle}{B_\phi^2/\mu_0} = \frac{\beta_0}{2}, \tag{322}$$

where $\langle\cdots\rangle$ denotes a volume average, as well as the *normal beta* parameter

$$\beta_N = 40\,\pi\,\frac{\beta\,a\,B_\phi}{\mu_0\,I_\phi} = 10\,\frac{\beta_0\,q_a}{\epsilon}, \tag{323}$$

where $I_\phi = 2\pi B_\phi\,a^2/(\mu_0 R_0\,q_a)$ is the toroidal plasma current.[1] Finally, the *magnetic Prandtl number* of the plasma is defined

$$P = \frac{\mu_0\,\mu}{\rho\,\eta} = 0.430\,\frac{\tau_R}{\tau_M}. \tag{324}$$

B. Nonlinear coupling of three neoclassical tearing modes

Consider the non-linear phase locking of three neoclassical tearing modes whose mode numbers are m_1, n_1; m_2, n_2; and m_3, n_3, where $m_3 = m_1 + m_2$ and $n_3 = n_1 + n_2$. As discussed in Sec. IV G, the phase-locking criterion is $F \geq 1$, where

$$F = \frac{\beta_N^7}{\hat\omega_0^2\,P\,\epsilon^{3/2}}\,\hat F_1(m_1,n_1;m_2,n_2;q_0,q_a,q_b). \tag{325}$$

Here, $\hat\omega_0 = \omega_0\,\tau_H$, and

$$\hat F_1 = \frac{7.7\times10^{-4}}{q_a^9}\left[n_1^2\ln\left(\frac{\hat r^{\,m_3,n_3}}{\hat r^{\,m_1,n_1}}\right) + n_2^2\ln\left(\frac{\hat r^{\,m_2,n_2}}{\hat r^{\,m_3,n_3}}\right)\right] \times(\bar m - 1 - \bar n\,q_0)^2(\mathcal{A}^{m_1,n_1}\,\mathcal{A}^{m_2,n_2}\,\mathcal{A}^{m_3,n_3})^2\hat{\mathcal{W}}. \tag{326}$$

Furthermore

$$\hat{\mathcal{W}} = \frac{(\hat w^{\,m_2,n_2})^4\,(\hat w^{m_3,n_3})^4}{(\hat r^{\,m_1,n_1})^2\,\hat w^{\,m_1,n_1}} + \frac{(\hat w^{\,m_1,n_1})^4\,(\hat w^{m_3,n_3})^4}{(\hat r^{\,m_2,n_2})^2\,\hat w^{\,m_2,n_2}} + \frac{(\hat w^{\,m_1,n_1})^4\,(\hat w^{m_2,n_2})^4}{(\hat r^{\,m_3,n_3})^2\,\hat w^{\,m_3,n_3}}, \tag{327}$$

and

$$\hat w^{\,m,n} = \left(\frac{m}{n}\right)^2\frac{\sqrt{\hat r^{\,m,n}}}{(-E^{m,n})}. \tag{328}$$

Finally, $\hat r^{\,m,n}$ is specified in Eq. (63), $E^{m,n}$ in Eq. (67), $\bar m$ in Eq. (72), $\bar n$ in Eq. (73), and $\mathcal{A}^{m,n}$ in Eq. (75).

According to Eq. (325), the nonlinear phase locking of three neoclassical tearing modes with different poloidal and toroidal mode numbers is greatly facilitated by increasing β_N, but is impeded by increasing differential plasma rotation (parameterized by $\hat\omega_0$) and plasma viscosity (parameterized by P). Figure 1 shows $\hat F_1(m_1,n_1;m_2,n_2;q_0,q_a,q_b)$ evaluated as a

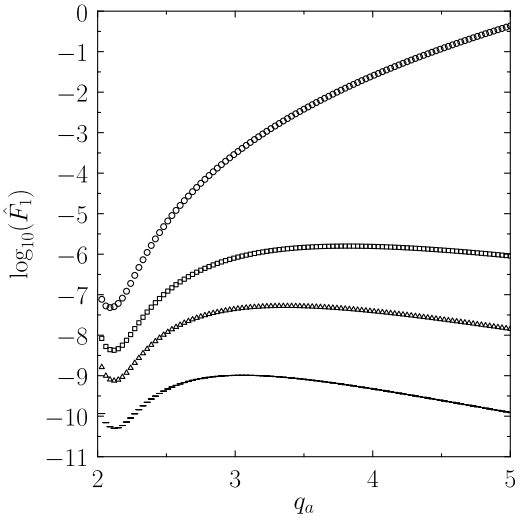

FIG. 1. $\hat F_1(m_1,n_1;m_2,n_2;q_0,q_a,q_b)$ calculated as a function of q_a for $m_1 = 2$, $n_1 = 1$, $m_2 = 3$, $n_2 = 2$, and $q_b = q_a$. The various curves correspond to $q_0 = 0.8$, 0.9, 0.95, and 1.0, respectively, in order from the bottom to the top.

function of q_0 and q_a for the nonlinear phase locking of the 2, 1, the 3, 2, and the 5, 3 neoclassical tearing modes in a fixed boundary plasma (i.e., $q_b = q_a$). It can be seen that $\hat{F}_1$ increases very strongly with increasing q_0. Moreover, at high q_0, $\hat{F}_1$ also increases strongly with increasing q_a. This indicates that the nonlinear phase locking of three neoclassical tearing modes in a tokamak plasma is greatly facilitated by increasing q_0, and, facilitated to a lesser extent by increasing q_a.

C. Toroidal coupling of two neoclassical tearing modes

Consider the toroidal phase locking of two neoclassical tearing modes whose mode numbers are m, n and $m+1, n$. As discussed in Sec. V G, the phase-locking criterion is $F \geq 1$, where

$$F = \frac{\beta_N^3\, \epsilon^{1/2}\, \left(\Delta_a^{1,0}\right)^2}{\hat{\omega}_0^2\, P}\, \hat{F}_2(m,n;q_0,q_a,q_b). \tag{329}$$

Here

$$\hat{F}_2 = \frac{6.8\times 10^{-2}}{q_0\, q_a^4}\left[n^2 \ln\left(\frac{\hat{r}^{\,m+1,n}}{\hat{r}^{\,m,n}}\right)\right] \times (\bar{m} - 1 - \bar{n}\, q_0)^2\, \left(\mathcal{A}^{m,n}\, \mathcal{A}^{m+1,n}\right)^2\, \hat{\mathcal{W}}, \tag{330}$$

where

$$\hat{\mathcal{W}} = \frac{\left(\hat{w}^{\,m+1,n}\right)^4}{\left(\hat{r}^{\,m,n}\right)^2\, \hat{w}^{\,m,n}} + \frac{\left(\hat{w}^{\,m,n}\right)^4}{\left(\hat{r}^{\,m+1,n}\right)^2\, \hat{w}^{\,m+1,n}}. \tag{331}$$

Finally, $\hat{r}^{\,m,n}$ is specified in Eq. (63), $E^{m,n}$ in Eq. (67), $\mathcal{A}^{m,n}$ in Eq. (75), $\bar{m}$ in Eq. (195), $\bar{n}$ in Eq. (196), and $\hat{w}^{\,m,n}$ in Eq. (328).

According to Eq. (329), the toroidal phase locking of two neoclassical tearing modes with the same toroidal mode number is facilitated by increasing β_N, and increasing Shafranov shift (parameterized by $\Delta_a^{1,0}$), but is impeded by increasing differential plasma rotation (parameterized by $\hat{\omega}_0$) and plasma viscosity (parameterized by P). Figure 2 shows $\hat{F}_2(m,n;q_0,q_a,q_b)$ evaluated as a function of q_0 and q_a for the toroidal phase locking of the 2, 1 and the 3, 1 neoclassical tearing modes in a fixed boundary plasma (i.e., $q_b = q_a$). As before, it can be seen that $\hat{F}_2$ increases very strongly with increasing q_0, and, at high q_0, also increases strongly with increasing q_a, which indicates that the toroidal phase locking of two neoclassical tearing modes is greatly facilitated by increasing q_0, and, facilitated to a lesser extent by increasing q_a. Note that $\hat{F}_2$ is significantly larger than $\hat{F}_1$, which simply indicates that conventional toroidal coupling is a much stronger effect in tokamak plasmas than nonlinear three-wave coupling.

D. Nonlinear toroidal coupling of two neoclassical tearing modes

Consider the nonlinear toroidal phase locking of two neoclassical tearing modes whose mode numbers are

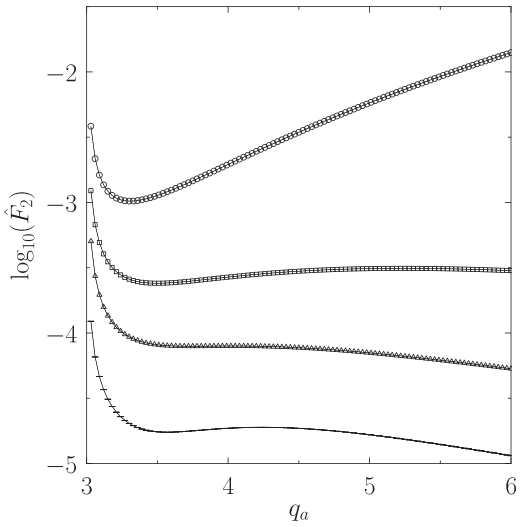

FIG. 2. $\hat{F}_2(m,n;q_0,q_a,q_b)$ calculated as a function of q_a for $m=2$, $n=1$, and $q_b = q_a$. The various curves correspond to $q_0 = 0.8$, 0.9, 0.95, and 1.0, respectively, in order from the bottom to the top.

$2m-1, 2n$ and m, n. As discussed in Sec. VI G, the phase-locking criterion is $F \geq 1$, where

$$F = \frac{\beta_N^7\, \left(\Delta_a^{1,0}\right)^2}{\hat{\omega}_0^2\, P\, \epsilon^{3/2}}\, \hat{F}_3(m,n;q_0,q_a,q_b). \tag{332}$$

Here

$$\hat{F}_3 = \frac{7.0\times 10^{-3}}{q_0\, q_a^8}\left[n^2 \ln\left(\frac{\hat{r}^{\,m,n}}{\hat{r}^{\,2m-1,2n}}\right)\right] \frac{(\bar{m} - 1 - \bar{n}\, q_0)^4}{\left(-E^{2m,2n}\right)^2} \times \left[\left(\mathcal{A}^{m,n}\right)^2 \left(\mathcal{A}^{2m,2n}\right)^2\, \mathcal{A}^{2m-1,2n}\right]^2\, \hat{\mathcal{W}}, \tag{333}$$

where

$$\hat{\mathcal{W}} = \frac{\left(\hat{w}^{\,m,n}\right)^8}{\left(\hat{r}^{\,2m-1,2n}\right)^2\, \hat{w}^{\,2m-1,2n}} + \frac{2\left(\hat{w}^{\,2m-1,2n}\right)^4 \left(\hat{w}^{\,m,n}\right)^3}{\left(\hat{r}^{\,m,n}\right)^2}. \tag{334}$$

Finally, $\hat{r}^{\,m,n}$ is specified in Eq. (63), $E^{m,n}$ in Eq. (67), $\mathcal{A}^{m,n}$ in Eq. (75), $\bar{m}$ in Eq. (263), $\bar{n}$ in Eq. (264), and $\hat{w}^{\,m,n}$ in Eq. (328). Note that we are neglecting the distinction between $\tilde{E}^{\,2m-1,2n}$ and $E^{2m-1,2n}$, as well as that between $\tilde{E}^{\,m,n}$ and $E^{m,n}$ [see Eqs. (259) and (260)]. This is a reasonable approximation provided that the island widths, as well as the Shafranov shift, are small compared to the plasma minor radius.

According to Eq. (332), the nonlinear toroidal phase locking of two neoclassical tearing modes with different poloidal and toroidal mode numbers is greatly facilitated by increasing β_N, and facilitated to a lesser extent by increasing Shafranov shift (parameterized by $\Delta_a^{1,0}$), but is impeded by increasing differential plasma rotation (parameterized by $\hat{\omega}_0$) and plasma viscosity (parameterized by P). Figure 3 shows $\hat{F}_3(m,n;q_0,q_a,q_b)$ evaluated as a function of q_0 and q_a for the nonlinear toroidal phase locking of the 2, 1 and the 3, 2 neoclassical tearing modes in a fixed boundary plasma (i.e., $q_b = q_a$). As before, it can be seen that $\hat{F}_3$ increases very strongly with increasing q_0, and, at high q_0, also increases strongly with increasing q_a, which indicates that

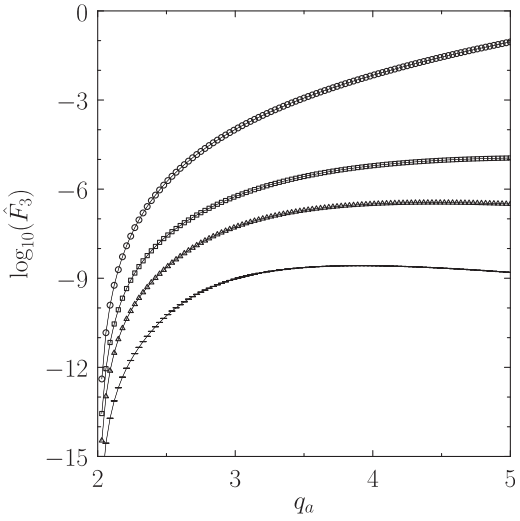

FIG. 3. $\hat{F}_3(m,n;q_0,q_a,q_b)$ calculated as a function of q_a for $m=2$, $n=1$, and $q_b=q_a$. The various curves correspond to $q_0=0.8$, 0.9, 0.95, and 1.0, respectively, in order from the bottom to the top.

the nonlinear toroidal phase locking of two neoclassical tearing modes is greatly facilitated by increasing q_0, and, facilitated to a lesser extent by increasing q_a. Note that $\hat{F}_3$ is significantly smaller than $\hat{F}_2$, which simply indicates that conventional toroidal coupling is a much stronger effect in tokamak plasmas than nonlinear toroidal coupling.

VIII. SUMMARY AND DISCUSSION

In this paper, we have investigated three distinct coupling mechanisms that can lead to the eventual phase locking of multiple neoclassical tearing modes in a tokamak plasma.

The first mechanism is the nonlinear three-wave coupling of three neoclassical tearing modes whose mode numbers are m_1, n_1; m_2, n_2; and $m_3=m_1+m_2, n_3=n_1+n_2$ (see Sec. IV). We find that there is a bifurcation to a phase-locked state when the mode amplitudes exceed a threshold value such that the frequency mismatch between the three modes is reduced to one half of its unperturbed value. The modes phase lock in the most mutually destabilizing possible phase relation. Moreover, the phase-locked state is such that one of the X-points of all three of the magnetic island chains associated with the different modes coincides permanently at a particular angular location that rotates both poloidally and toroidally. Note that this type of phase locking is fairly unlikely to occur in tokamaks, because it requires three neoclassical tearing modes (that just happen to satisfy the three-wave coupling constraint $m_3=m_1+m_2, n_3=n_1+n_2$) to be present simultaneously in the plasma, which would be a very unusual occurrence.

The second mechanism is the conventional toroidal coupling of two neoclassical tearing modes whose mode numbers are m, n and $m+1,n$ (see Sec. V). This type of coupling can be treated as a form of nonlinear three-wave coupling in which one of the three coupled modes is the 1, 0 component of the plasma equilibrium associated with the Shafranov shift. We find that there is a bifurcation to a phase-locked state when the mode amplitudes exceed a threshold value such that the frequency mismatch between the m, n and the $m+1,n$ modes is reduced to one half of its unperturbed value. The modes phase lock in the most mutually destabilizing possible phase relation. Moreover, the phase-locked state is such that one of the X-points of the magnetic island chains associated with the m, n and the $m+1,n$ modes coincides permanently at an angular position on the outboard mid-plane that rotates toroidally. Finally, the phase-locked state is characterized by a modified toroidal angular velocity profile, internal to the $m+1,n$ rational surface, which is either flattened or inverted (depending on the amount of poloidal flow present in the plasma). Toroidal coupling of tearing modes with the same toroidal mode number, and poloidal mode numbers differing by unity, is frequently observed in tokamak plasmas.[43] Moreover, in accordance with our analysis, the observed phase-locked state is such that one of the X-points of the coupled island chains coincides permanently on the outboard mid-plane at an angular location that rotates toroidally.[43]

The third mechanism is the nonlinear toroidal coupling of two neoclassical tearing modes whose mode numbers are m, n and $2m-1,2n$ (see Sec. VI). This coupling takes place in two stages. First, the m, n mode coupled nonlinearly to itself to produce the $2m,2n$ mode. Second, the $2m,2n$ mode couples toroidally to the $2m-1,2n$ mode. We find that there is a bifurcation to a phase-locked state when the mode amplitudes exceed a threshold value such that the frequency mismatch between the $2m-1,2n$ and the $2m,2n$ modes is reduced to one half of its unperturbed value. The modes phase lock in the most mutually destabilizing possible phase relation. Moreover, the phase-locked state is such that one of the X-points of the magnetic island chains associated with the m, n and the $2m-1,2n$ modes coincides permanently at an angular position on the outboard mid-plane that rotates toroidally. Finally, the phase-locked state is characterized by a modified toroidal angular velocity profile, internal to the m, n rational surface, which is either flattened or inverted (depending on the amount of poloidal flow present in the plasma). The nonlinear toroidal coupling of the 2, 1 and the 3, 2 neoclassical tearing modes has been observed on both JET and DIII-D.[21,22] In accordance with our analysis, the phase-locking bifurcation is observed to take place when the frequency mismatch between the 3, 2 and the 4, 2 modes has been reduced to about one half of its original value. Moreover, the phase-locked state is characterized by a toroidal angular velocity profile, internal to the 2, 1 rational surface, which is either flattened or inverted. In further accordance, the phase-locked state is such that one of the X-points of the 3, 2 and 2, 1 island chains coincides permanently on the outboard mid-plane at an angular location that rotates toroidally.

ACKNOWLEDGMENTS

This research was funded by the U.S. Department of Energy under Contract No. DE-FG02-04ER-54742.

[1]J. A. Wesson, *Tokamaks*, 4th ed. (Oxford University Press, Oxford, 2012).
[2]J. P. Freidberg, *Ideal Magnetohydrodynamics* (Springer, Berlin, 1987).
[3]J. A. Wesson, Nucl. Fusion **18**, 87 (1978).
[4]H. P. Furth, J. Killeen, and M. N. Rosenbluth, Phys. Fluids **6**, 459 (1963).

[5]P. H. Rutherford, Phys. Fluids **16**, 1903 (1973).
[6]A. Thyagaraja, Phys. Fluids **24**, 1716 (1981).
[7]D. F. Escande and M. Ottaviani, Phys. Lett. A **323**, 278 (2004).
[8]R. J. Hastie, F. Militello, and F. Porcelli, Phys. Rev. Lett. **95**, 065001 (2005).
[9]Z. Chang and J. D. Callen, Nucl. Fusion **30**, 219 (1990).
[10]R. Carrera, R. D. Hazeltine, and M. Kotschenreuther, Phys. Fluids **29**, 899 (1986).
[11]R. Fitzpatrick, Phys. Plasmas **2**, 825 (1995).
[12]R. J. Buttery, S. Günter, G. Giruzzi, T. C. Hender, D. Howell, G. Huysmans, R. J. La Haye, M. Maraschek, H. Reimerdes, O. Sauter, C. D. Warrick, H. R. Wilson, and H. Zohm, Plasma Phys. Controlled Fusion **42**, B61 (2000).
[13]Q. Yu, S. Günter, K. Lackner, A. Gude, and M. Maraschek, Nucl. Fusion **40**, 2031 (2000).
[14]Z. Chang, J. D. Callen, E. D. Fredrickson, R. V. Budny, C. C. Hegna, K. M. McGuire, M. C. Zarnstorff, and the TFTR Group, Phys. Rev. Lett. **74**, 4663 (1995).
[15]R. J. La Haye, L. L. Lao, E. J. Strait, and T. S. Taylor, Nucl. Fusion **37**, 397 (1997).
[16]The JET Team, Nucl. Fusion **39**, 1965 (1999).
[17]O. Gruber, R. C. Wolf, R. Dux, C. Fuchs, S. Günter, A. Kallenbach, K. Lackner, M. Maraschek, P. J. McCarthy, H. Meister, G. Pereverzev, F. Ryter, J. Schweinzer, U. Seidel, S. Sesnic, A. Stäbler, J. Stober, and the ASDEX Upgrade Team, Phys. Rev. Lett. **83**, 1787 (1999).
[18]T. C. Luce, M. R. Wade, P. A. Politzer, S. L. Allen, M. E. Austin, D. R. Baker, B. Bray, D. P. Brennan, K. H. Burrell, T. A. Casper, M. S. Chu, J. C. DeBoo, E. J. Doyle, J. R. Ferron, A. M. Garofalo, P. Gohil, I. A. Gorelov, C. M. Greenfield, R. J. Groebner, W. W. Heidbrink, C.-L. Hsieh, A. W. Hyatt, R. Jayakumar, J. E. Kinsey, R. J. La Haye, L. L. Lao, C. J. Lasnier, E. A. Lazarus, A. W. Leonard, Y. R. Lin-Liu, J. Lohr, M. A. Mahdavi, M. A. Makowski, M. Murakami, C. C. Petty, R. I. Pinsker, R. Prater, C. L. Rettig, T. L. Rhodes, B. W. Rice, E. J. Strait, T. S. Taylor, D. M. Thomas, A. D. Turnbull, J. G. Watkins, W. P. West, and K.-L. Wong, Nucl. Fusion **41**, 1585 (2001).
[19]M. R. Wade, T. C. Luce, R. J. Jayakumar, P. A. Politzer, A. W. Hyatt, J. R. Ferron, C. M. Greenfield, M. Murakami, C. C. Petty, R. Prater, J. C. DeBoo, R. J. La Haye, P. Gohil, and T. L. Rhodes, Nucl. Fusion **45**, 407 (2005).
[20]A. C. C. Sips, G. Tardini, C. B. Forest, O. Gruber, P. J. Mc Carthy, A. Gude, L. D. Horton, V. Igochine, O. Kardaun, C. F. Maggi, M. Maraschek, V. Mertens, R. Neu, A. G. Peeters, G. V. Pereverzev, A. Stäbler, J. Stober, W. Suttrop, and the ASDEX Upgrade Team, Nucl. Fusion **47**, 1485 (2007).
[21]T. C. Hender, D. F. Howell, R. J. Buttery, O. Sauter, F. Sartori, R. J. La Haye, A. W. Hyatt, C. C. Petty, the JET EFDA Contributors, and the DIII-D Team, Nucl. Fusion **44**, 788 (2004).
[22]B. Tobias, B. A. Grierson, C. M. Muscatello, X. Ren, C. W. Dornier, N. C. Luhmann, Jr., S. E. Zemedkun, T. L. Munsat, and I. G. J. Classen, Rev. Sci. Instrum. **85**, 11D847 (2014).
[23]E. Alessi, P. Buratti, E. Giovannozzi, G. Pucella, and the JET EDFA Contributors, in *Proceedings of 14th European Physical Society Conference on Plasma Physics* (2014), No. P1.028.
[24]C. C. Hegna, Phys. Plasmas **3**, 4646 (1996).
[25]R. M. Coelho, E. Lazzaro, M. F. Nave, and F. Serra, Phys. Plasmas **6**, 1194 (1999).
[26]R. Fitzpatrick, Phys. Plasmas **6**, 1168 (1999).
[27]J. W. Connor, S. C. Cowley, R. J. Hastie, T. C. Hender, A. Hood, and T. J. Martin, Phys. Fluids **31**, 577 (1988).
[28]J. W. Connor, R. J. Hastie, and J. B. Taylor, Phys. Fluids B **3**, 1532 (1991).
[29]R. Fitzpatrick, R. J. Hastie, T. J. Martin, and C. M. Roach, Nucl. Fusion **33**, 1533 (1993).
[30]R. Fitzpatrick, Nucl. Fusion **33**, 1049 (1993).
[31]R. Fitzpatrick, Phys. Plasmas **1**, 3308 (1994).
[32]R. Fitzpatrick, Phys. Plasmas **5**, 3325 (1998).
[33]R. Fitzpatrick, Phys. Plasmas **10**, 2304 (2003).
[34]E. Poli, A. G. Peeters, A. Bergmann, S. Günter, and S. D. Pinches, Phys. Rev. Lett. **88**, 075001 (2002).
[35]M. Kotschenreuther, R. D. Hazeltine, and P. J. Morrison, Phys. Fluids **28**, 294 (1985).
[36]T. H. Stix, Phys. Fluids **16**, 1260 (1973).
[37]R. Fitzpatrick, Phys. Plasmas **21**, 092513 (2014).
[38]Q. Hu, Q. Yu, B. Rao, Y. Ding, X. Hu, G. Zhuang, and the J-TEXT Team, Nucl. Fusion **52**, 083011 (2012).
[39]R. J. La Haye, T. N. Carlstrom, R. R. Goforth, G. L. Jackson, M. J. Schaffer, T. Tamano, and P. L. Taylor, Phys. Fluids **27**, 2576 (1984).
[40]T. Tamano, W. D. Boyd, C. Chu, Y. Kondoh, R. J. La Haye, P. S. Lee, M. Saito, M. J. Schaffer, and P. L. Taylor, Phys. Rev. Lett. **59**, 1444 (1987).
[41]K. Hattori, Y. Hirano, T. Shimada, Y. Yagi, Y. Maejima, I. Hirota, and K. Ogawa, Phys. Fluids B **3**, 3111 (1991).
[42]R. Fitzpatrick and P. Zanca, Phys. Plasmas **9**, 2707 (2002).
[43]W. Suttrop, K. Büchl, J. C. Fuchs, M. Kaufmann, K. Lackner, M. Maraschek, V. Mertens, R. Neu, M. Schittenhelm, M. Sokoll, H. Zohm, and the Asdex Upgrade Team, Nucl. Fusion **37**, 119 (1997).